Dual Thermo- and pH-Responsive Block Copolymer of Poly(N -isopropylacrylamide)- block -Poly(N , N -diethylamino Ethyl Acrylamide): Synthesis, Characterization, Phase Transition, and Self-Assembly Behavior in Aqueous Solution

Fang Yin, Pascale Laborie, Barbara Lonetti, Stéphane Gineste, Yannick Coppel, Nancy Lauth-de Viguerie, Jean-Daniel Marty

Dual thermo- and pH-responsive block copolymer of poly(*N*-isopropylacrylamide)-block-poly(*N*,*N*-diethylamino ethyl acrylamide): synthesis, characterization, phase transition and self-assembly behavior in aqueous solution

Fang Yin,[a] *Pascale Laborie,*[a] *Barbara Lonetti,*[a] *Stéphane Gineste,*[a] *Yannick Coppel,*[b] *Nancy Lauth-de Viguerie*[a,]* *and Jean-Daniel Marty*[a,]*

[a] Laboratoire des IMRCP, Université de Toulouse, CNRS UMR 5623, Université Toulouse III – Paul Sabatier, 118 route de Narbonne, 31062 Toulouse, France.

[b] Laboratoire de Chimie de Coordination, Université de Toulouse, CNRS UPR 8241, Université Toulouse III – Paul Sabatier, 205 route de Narbonne, 31077 Toulouse, France.

KEYWORDS. Block copolymers, PNIPAM, Stimuli-responsive polymer, pH-responsive polymers, PDEAEMA

Table of Content

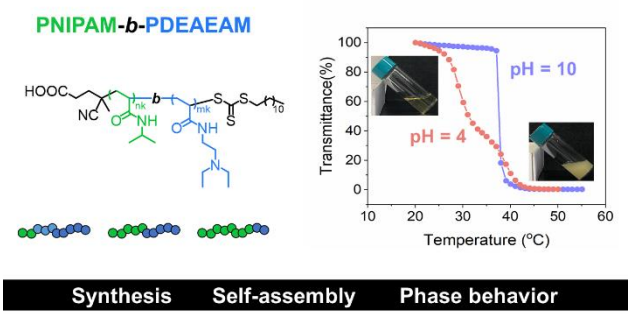

ABSTRACT. Doubly thermo- and pH-responsive poly(*N*-isopropylacrylamide)-*block*-poly(*N*,*N*-diethylamino ethyl acrylamide) (PNIPAM-*b*-PDEAEAM) with different compositions were synthesized by reversible addition-fragmentation chain-transfer (RAFT) polymerization. The properties of these polymers and corresponding homopolymers in solution (solubility, self-assembly behavior) depend on the value of pH and the protonation degree of diethylamino moiety. The effect of the nature of the polymer chain ends also appears to be critical to fully understand this behavior. At pH 10, both PNIPAM and PDEAEAM blocks are thermoresponsive and make a cooperative contribution to phase transition, stable spherical nanoobjects are detected as temperature rises over transition point. At pH 4, PNIPAM-*b*-PDEAEAM with longer PDEAEAM length displays a two-step thermoresponsive behavior; upon heating, PNIPAM chains undergo shrinkage and subsequent reorganization causing the formation of large aggregates with a positively charged shell made of PDEAEAM block in its protonated state. The aggregation processes are also particularly sensitive to kinetic considerations and therefore measured size of aggregates depends strongly on the history of polymer solution.

1. Introduction

Stimuli-responsive polymers[1-3] have been extensively studied due to their ability to respond macroscopically, rapidly and reversibly to changes in their local environment. External stimuli such as temperature, pH, electric or magnetic fields, light… alter molecular interactions near critical points and modify the conformations of polymer chains in solution, allowing these polymers to have promising applications in areas ranging from material science to biology.[4-6]

One of the most significant class of stimuli-responsive polymers are thermo-responsive polymers.[7-9] They exhibit a soluble-to-insoluble phase transition at a lower critical temperature (LCST) or an insoluble-to-soluble phase transition at upper critical solution temperature (UCST). Different families of LCST-type polymers have been described based on the polymerization of *N*-isopropylacrylamide (NIPAM),[10,11] *N*,*N*-diethylacrylamide (DEAAM), *N*-vinylcaprolactam (VCL),[12-15] 2-(2-methoxyethoxy) ethyl methacrylate (MEO_2MA) or methylvinylether (MVE)[16] (**Scheme S1**). Among them, polymers based on *N*-alkyl substituted poly(acrylamide)s like PNIPAM have been the most studied. The nature of substituted *N*-alkyl group is a key factor to determine the behavior of these polymers in solution: poly(*N*,*N*-dimethylacrylamide) (PDMA) is fully soluble in water, PNIPAM and poly(*N*,*N*-diethylacrylamide) (PDEAAM) have similar LCSTs around 32 °C and poly(*N*-*n*-butylacrylamide) (PNNBAM) is insoluble in water (**Scheme 1A**). More recently, numerous investigations have focused on homopolymers bearing a tertiary amine function grafted on poly((meth)acrylamide)s and poly((meth)acrylate)s as illustrated in **Scheme 1B**.[17,18]

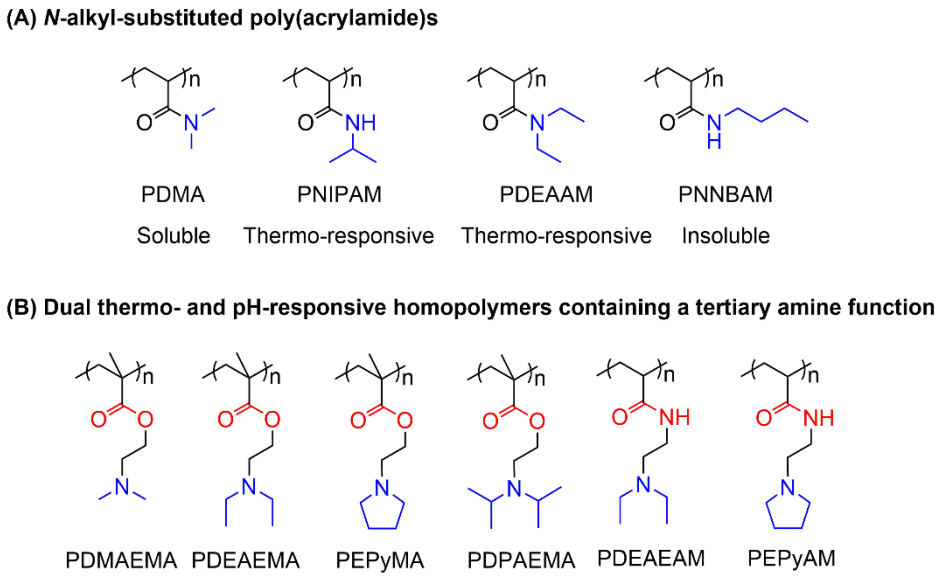

Scheme 1. Chemical structures of (A) *N*-alkyl-substituted poly(acrylamide)s and (B) Dual thermo- and pH-responsive homopolymers containing a tertiary amine function. (PDMA: poly(*N*,*N*-dimethylacrylamide), PNIPAM: poly(*N*-isopropylacrylamide), PDEAAM: poly(*N*,*N*-diethylacrylamide), PNNBAM: poly(*N*-*n*-butylacrylamide), PDMAEMA: poly(2-(dimethylamino)ethyl methacrylate), PDEAEMA: poly(2-(diethylamino)ethyl methacrylate), PEPyMA: poly(*N*-ethylpyrrolidine methacrylate), PDPAEMA: poly(2-(diisopropylamino) ethyl methacrylate), PDEAEAM: poly(*N*,*N*-diethylamino ethyl acrylamide), PEPyAM: poly(*N*-ethylpyrrolidine acrylamide).

Thanks to the reversible protonation-deprotonation transition of these tertiary amines and the nature of alkyl substituted group, these polymers therefore exhibit either pH- or dual pH-/thermo- responsive properties.[19,20] Among them, poly(*N*,*N*-(dimethylamino)ethyl methacrylate) (PDMAEMA) (p*K*a ~ 7.5) and poly(*N*,*N*-

(diethylamino)ethyl methacrylate) (PDEAEMA) (p*K*a ~ 7.4) are weak polybases, partially protonated in a physiological solution and are the most studied thermo-/pH-responsive polymers since their corresponding monomers are commercially available. Beyond the degree of polymerization of the polymer studied, the number of carbon atoms in the alkyl substituent (methyl or ethyl) has a pronounced effect on the value of the LCST: PDMAEMA is well soluble in water at room temperature whatever the pH value and presents a LCST behavior only at high pH values (above p*K*a). In contrast, PDEAEMA shows an LCST-type phase behavior at pH 6 – 7 and is hardly soluble for a pH value higher than 8: hence its T_c value ranges from 69 to 30 °C as pH changes from 6.5 to 8. This makes PDMAEMA a very promising polymer to be used in various applications including gene transfer agent and drug delivery systems.[21-23] Besides these families of homopolymers, multi-responsive polymer structures have been obtained from the copolymerization (block or random) of two or more stimuli-responsive monomers. Hence, diblock copolymers comprising a thermoresponsive block based on thermoresponsive PNIPAM and a pH-responsive block based on poly((meth)acrylate)s, e.g. poly(2-(dimethylamino)ethyl acrylate) (PDMAEA),[24] PDMAEMA,[25-26] or PDEAEMA,[25] have previously reported and present tunable self-assembly properties in aqueous media upon variation of pH and/or temperature. For example, $PNIPAM_{232}$-*b*-$PDEAEMA_{106}$ exhibits intriguing micellization behavior in aqueous solution. At room temperature, the copolymer chains molecularly dissolve at pH < 6.5 and form PDEAEMA-core micelles at pH > 7.5. Above the LCST of the PNIPAM block,

copolymer chains self-assemble into structurally inverted PNIPAM-core micelles at pH < 6.5.

We aim here at studying block polymer structures based on PNIPAM associated with monomer comprising tertiary amine functions. For this purpose, *N*,*N*-diethylamino)ethyl acrylamide (DEAEAM) is a monomer of choice. Whereas it is closely related to the most commonly studied methacrylate-based polymer PDEAEMA, it comprises an amide function that gives to this monomer numerous advantages compared to corresponding methacrylate: a higher hydrolytic stability during heating/cooling cycles at different pH values and reactivity ratio closely related to the one of NIPAM. PDEAEAM is thermoresponsive in its unprotonated form and lose this property in its protonated form. Its T_c value ranges from 50.2 to 33.1 °C as pH changes from 8.5 to 11.0.[27, 28] The use of DEAEAM was scarcely studied in literature for the formation of different copolymer. e.g. Guan and co-workers designed a multi-stimuli responsive star polymer with aggregation-induced effect, which displayed a good performance in long-term cell tracing.[29] Kim et al. employed P(DEAEAM-*ran*-NIPAM) as responsive surfactant to modulate shape transition of poly(styrene)-*b*-poly(4-vinylpyridine) particles between football and lens over a subtle change of temperature and pH.[30]

In this work, the objective is to evaluate how copolymer composition and architecture affect the thermoresponsive properties and the aggregation behavior of a family of block copolymers issued form the copolymerization of DEAEAM and NIPAM

(**Scheme 2**). Their synthesis was performed by reversible addition-fragmentation chain transfer (RAFT) polymerization. The behavior (solubility, self-assembly process…) of these block copolymers in aqueous media was studied as a function of pH and temperature. We highlighted the critical roles of the copolymer composition, pH and of the nature of chain ends on the colloidal properties (solubility and aggregation process) of these polymers in solution.

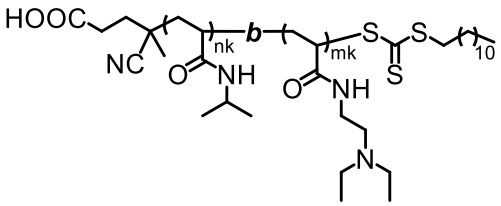

Scheme 2. Structure of PNIPAM-*b*-PDEAEAM copolymer (noted in the following as PN-*b*-PD) presenting dual thermo/pH responsiveness.

2. Experimental Section

2.1. Materials.

N-isopropylacrylamide (NIPAM, Sigma-Aldrich), *N*,*N*-diethylethylenediamine (≥ 99%, Sigma-Aldrich), acryloyl chloride (≥ 97%, Sigma-Aldrich), 4-cyano-4-[(dodecylsulfanylthiocarbonyl) sulfanyl] pentanoic acid (CDTPA, 97%, Sigma-Aldrich), triethylamine (TEA, 99%, Lancaster) were used as received. 2,2'-Azobis(isobutyronitrile) (AIBN) was crystallized twice from methanol. 1,4-dioxane and chloroform were purified by passing through alumina columns prior to use. All other reagents were used as received without further purification. Deionized water used

in all experiments was purified through a filter and ion exchange resin using a Purite device with a resistivity of 18.2 MΩ·cm.

2.2. Characterization methods.

Nuclear Magnetic Resonance (NMR), size exclusion chromatography (SEC), Fourier transform infrared (FT-IR), turbidimetry measurement, dynamic Light Scattering (DLS),[31] Differential Scanning Calorimetry (DSC), surface tension measurements, determination of pKa, Transmission Electron Microscopy (TEM) and Freeze-Fracture transmission electron microscopy (FF-TEM) were described in section 1 of electronic supporting information.

Small Angle X-rays scattering (SAXS) on 1 wt.% PN_{5k}-*b*-PD_{5k} solution at pH 4 and pH 9 was performed with a XEUSS 2.0 SAXS/WAXS laboratory beamline equipped with a Cu source (E = 8 keV). The 2D SAXS patterns were collected using a pixel detector PILATUS3 1 M from Detrics. The sample to detector distance was 1216.5 mm (beam size 0.8 × 0.8 mm), covering a q-range from 0.007 to 0.5 $Å^{-1}$. q is the scattering wave vector defined as $q = (4\pi/\lambda)\sin\theta/2$, λ is the wavelength ($\lambda \sim 1.54$ Å) and θ is the scattering angle. The solutions were loaded in borosilicate capillaries of 1.5 mm diameter in thermostatic sample holders. The SAXS curves have been measured at 25 and 60 °C. The normalized scattering intensity for non-interacting polydisperse objects is given by:

$$I(q) = \int_0^\infty P(q,R)f(R)dR \quad \textbf{(eq. 1)}$$

$f(R)$ is the size distribution function, which in our case is a Schulz size distribution function with

$$f(R) = \left(\frac{Z+1}{\bar{R}}\right)^{Z+1} \frac{R^Z}{\Gamma(Z+1)} exp\left(\frac{-Z+1}{\bar{R}}R\right) \textbf{ (eq. 2)}$$

with Z = 1/(1-p^2), with *p* the polydispersity and $\bar{R}$ the mean size. For spherical objects:

$$P(q,R) = (\frac{16}{9}\pi^2)\{(\Delta\rho)R^3\mathrm{F}(q\mathrm{R})\}^2 \textbf{ (eq. 3)}$$

$\Delta\rho$ is the difference between the scattering length density of the polymer and the solvent, and $\mathrm{F}(q\mathrm{R})$ is the scattering amplitude of a sphere of radius R:

$$F(q\mathrm{R}) = \frac{3[\sin(q\mathrm{R}) - q\mathrm{R}\cos(\mathrm{qR})]}{(q\mathrm{R})^3} \textbf{ (eq. 4)}$$

For block copolymer micelles, it is often necessary to consider an extra contribution at high-*q* vectors related to fluctuations originating from chain statistics and interchain interactions of polymer chains. This contribution is well reproduced by the Ornstein-Zernike type term:

$$P(q)=P_0(q)+I_o/(1+(q^2\zeta^2)^{d/2}) \textbf{ (eq. 5)}$$

Where ζ is the length scale of density fluctuations (order of nm) and d is related to the fractal dimension of the scattering chains. We fixed *d* to -1.6 as expected for swollen polymer chains in good solvent, ζ is 0.9 nm. The model used to describe the curves as star-like assemblies is the one developed for star-polymers formed of gaussian polymer arms:[32]

$$I(q) = \frac{2}{fv^2}\left[v - 1 + e^{-v} + \frac{f-1}{2}(1-e^{-v})^2\right] \textbf{ (eq. 6)}$$

$$v = \frac{\langle R_g^2 \rangle q^2 f}{(3f-2)} \quad \textbf{(eq. 7)}$$

with $\langle R_g^2 \rangle$ is the square of the ensemble average gyration radius of the full assembly and f is the number of arms of the self-assembly. Best fits of the form factor $P(q)$ for the measured data were derived using the SAXS utilities analysis package (**eq. 1** to **5**) for samples at pH 4 and SASView (**eq. 6-7**) for pH 10.

2.3. Synthesis.

Synthesis of (N,N-diethylamino) ethyl acrylamide monomer (DEAEAM). DEAEAM was prepared according a previously described procedure.[27] Briefly, *N*,*N*-diethylethylenediamine (60 mmol, 6.97 g), triethylamine (TEA, 72 mmol, 7.29 g) and $CHCl_3$ (100 mL) were added in a Schlenk flask under argon atmosphere in an ice-water bath. Acryloyl chloride (72 mmol, 6 mL) dissolved in $CHCl_3$ was added dropwise into flask within 1 h, after complete addition, the reaction was warmed up to room temperature for 4 h. Then the reaction mixture was washed with dilute NaOH solution and with deionized water three times, respectively. The organic phase was collected and concentrated under reduced pressure, the resulting residue was purified by aluminum oxide column chromatography (petroleum ether/ethyl acetate gradient 3:1 to 0:1, v/v) to give DEAEAM (5.39 g, yield: 53%). ^{1}H NMR (300 MHz, $CDCl_3$) δ_H (ppm): 6.43 (s, 1H, -N<u>H</u>-), 6.21 (dd, 1H, C<u>H</u>$_2$=CH-), 6.08 (dd, 1H, C<u>H</u>$_2$=CH-), 5.55 (dd, 1H, CH$_2$=C<u>H</u>-), 3.32 (q, 2H, -NH-C<u>H</u>$_2$-), 2.55-2.44 (m, 6H, -N(C<u>H</u>$_2$)$_3$), 0.96 (t, 6H, -C<u>H</u>$_3$) ; ^{13}C NMR (75 MHz, $CDCl_3$) δ_C (ppm): 165.51, 131.13, 125.78, 51.28, 46.68, 36.90 and 11.75 (**Figures S1**).

Synthesis of poly(N-isopropyl acrylamide) macro-RAFT agent (PN). In the case of PN_{5k}, a mixture of NIPAM (2 g, 17.674 mmol), AIBN (0.036 g, 0.218 mmol), CDTPA (0.176 g, 0.436 mmol) was dissolved in 1,4-dioxane (4.741 g) into a Schlenk flask under an argon flow. The flask was degassed through three freeze-pump-thaw cycles and placed in a preheated oil bath (75 °C). After 9 h, the reaction was quenched by a rapid immersion in liquid nitrogen. The obtained mixture was concentrated and precipitated in cold diethyl ether twice to remove unreacted monomer, followed by drying under vacuum to afford pure PN_{5k} (conversion: 99.9%). NIPAM conversion was calculated by comparing the integrals at 5.44 ppm corresponding to vinyl protons of the monomer to the one at 3.92 ppm corresponding to methyne in isopropyl group. $M_{n,NMR}$ was determined from ^{1}H NMR spectrum by comparing the signal areas at 0.85 ppm (RAFT terminal, -CH_3) and at 3.92 ppm (NIPAM, -CH- adjacent to -CH_3 group). $M_{n,theo}$ = 5000 g·mol^{-1}, $M_{n,NMR}$ = 6130 g·mol^{-1}. In DMF (containing 10 mM LiBr): $M_{n,SEC}$ = 6080 g·mol^{-1}, Đ = 1.06 ; In THF (containing 2 vol.% TEA): $M_{n,SEC}$ = 4720 g·mol^{-1}, Đ =1.03. ^{1}H NMR (500 MHz, D_2O) δ_H (ppm): 3.92 (s, 1H, -C<u>H</u>$(CH_3)_2$), 2.52 - 1.60 (m, -C<u>H</u>$_2$CH-CONH-, -CH_2C<u>H</u>-CONH-, -C(CN)(C<u>H</u>$_3$)-, -C<u>H</u>$_2$$CH_2$COOH, -$CH_2$C<u>H</u>$_2$COOH), 1.33 (s, 20H, -(C<u>H</u>$_2$)$_{10}$-CH_3), 1.16 (s, 6H, -CH(C<u>H</u>$_3$)$_2$), 0.85 (s, 3H, -$(CH_2)_{10}$-C<u>H</u>$_3$).

Synthesis of poly(N-isopropyl acrylamide)-block-poly(N,N-(diethylamino) ethyl acrylamide) (PN-b-PD). In the case of PN_{5k}-*b*-PD_{5k}, DEAEAM (2 g, 11.747 mmol), PN_{5k} (2 g, 0.4 mmol), AIBN (0.059 g, 0.36 mmol), 1,3,5-trioxane as an internal standard (0.106 g, 1.175 mmol) were dissolved in 1,4-dioxane (3.43 g) and placed into a Schlenk flask with a magnetic stirrer. After three freeze-pump-thaw cycles, the flask was

immersed in a preheated oil bath at 70 °C. The conversion of DEAEAM was determined from ^{1}H NMR analysis. Once the desired conversion was obtained, the polymerization was stopped by rapidly cooling in liquid nitrogen. The resulting mixture was precipitated in cold diethyl ether twice and dried under vacuum (conversion: 96.6%). $M_{n,NMR}$ was calculated on the basis of $M_{n,NMR}$ of PN_{5k}, as well as integral ratio of characteristic signal of PN at 3.90 ppm and that of PD at 3.32 ppm. $M_{n,theo}$ = 9840 g·mol^{-1}, $M_{n,NMR}$ = 11090 g·mol^{-1}. In DMF (containing 10 mM LiBr): $M_{n,SEC}$ = 8340 g·mol^{-1}, Đ = 1.09; in THF (containing 2 vol.% TEA): $M_{n,SEC}$ = 6860 g·mol^{-1}, Đ = 1.16. ^{1}H NMR (500 MHz, D_2O) δ_H (ppm): 3.90 (s, 1H, -C<u>H</u>$(CH_3)_2$), 3.32 (s, 2H, -CONH-C<u>H</u>$_2$-), 2.63 (s, 6H, -N(C<u>H</u>$_2)_3$), 2.02 - 1.33 (m, -C<u>H</u>$_2$CH-CONH-, -CH$_2$C<u>H</u>-CONH-, -C(CN)(C<u>H</u>$_3$)-, -C<u>H</u>$_2$CH$_2$COOH, -CH$_2$C<u>H</u>$_2$COOH), 1.25 (s, 20H, -(C<u>H</u>$_2)_{10}$-CH$_3$), 1.14 (s, 6H, -NHCH(C<u>H</u>$_3)_2$), 1.06 (s, 6H, -N(CH$_2$C<u>H</u>$_3)_2$), 0.85 (s, 3H, -(CH$_2)_{10}$-C<u>H</u>$_3$).

Synthesis of poly(N, N-(diethylamino) ethyl acrylamide) homopolymer (PD). In the case of PD_{5k}, DEAEAM (2 g, 11.747 mmol), AIBN (0.050 g, 0.305 mmol), CDTPA (0.176 g, 0.435 mmol), 1,3,5-trioxane (0.106 g, 1.175 mmol, as an internal standard) and 1,4-dioxane (3.497 g) were added into a Schlenk flask with a magnetic stirrer. The mixture was degassed by three freeze-pump-thaw cycles and placed in a preheated oil bath at 70 °C. After a given time, the polymerization was quenched by rapid immersion of flask in liquid nitrogen and the crude PD_{5k} was purified by dialysis against deionized water for three days and dried by lyophilization (conversion: 95.4%). $M_{n,NMR}$ was calculated by comparing integrals of the signal at 0.88 ppm (RAFT terminal, -CH$_3$) to the one of the signal at 3.33 ppm (DEAEAM, -CH$_2$- adjacent to -CONH- group) in ^{1}H

NMR spectrum. $M_{n,theo}$ = 4790 g·mol^{-1}, $M_{n,NMR}$ = 4810 g·mol^{-1}. In DMF (containing 10 mM LiBr): $M_{n,SEC}$ = 6900 g·mol^{-1}, Đ = 1.21; in THF (containing 2 vol.% TEA): $M_{n,SEC}$ = 4210 g·mol^{-1}, Đ = 1.09. ^{1}H NMR (500 MHz, D_2O) δ_H (ppm): 3.33 (s, 2H, -CONH-C$\underline{H}_2$-), 2.64 (s, 6H, -N(C$\underline{H}_2$CH$_3$)$_2$C$\underline{H}_2$-), 2.31 - 1.62 (m, -C$\underline{H}_2$CH-CONH-, -CH$_2$C$\underline{H}$-CONH-, -C(CN)(C$\underline{H}_3$)-, -C$\underline{H}_2$CH$_2$COOH, -CH$_2$C$\underline{H}_2$COOH), 1.26 (s, 20H, -(C$\underline{H}_2$)$_{10}$-CH$_3$), 1.08 (s, 6H, -N(CH$_2$C$\underline{H}_3$)$_2$), 0.88 (t, 3H, -(CH$_2$)$_{10}$-C$\underline{H}_3$).

PN, PD homopolymers with different molecular weights and block copolymers PN-*b*-PD varying copolymer compositions were also synthesized by using the similar polymerization procedure (feed ratios are summarized in **Table S1**), their corresponding ^{1}H NMR spectra are given in **Figures S2-S4**.

3. Results and Discussion.

3.1. Synthesis and characterization of homo- and copolymers.

The synthesis of the monomer DEAEAM was successfully achieved using a previously described protocol (**Figures S1**).[27] Well-defined thermo- and pH-responsive diblock copolymers comprising PNIPAM and PDEAEAM blocks were successfully synthesized by reversible addition-fragmentation chain transfer radical (RAFT)[33-35] polymerization using azobisisobutyronitrile (AIBN) as free-radical initiator and 4-cyano-4-[(dodecylsulfanylthiocarbony) sulfanyl] pentanoic acid (CDTPA) as a RAFT agent. This chain transfer agent was chosen due to its known reactivity for both monomers leading to a well control of polymerization.[27,34] It is noteworthy that CDTPA used introduced a dodecyl and a carboxyl terminal groups which can affect the properties of the polymers in solution (*vide infra*). Through tuning the feed ratio of monomer and CDTPA, a series of PNIPAM-*b*-PDEAEAM with different compositions were obtained: $PNIPAM_{2k}$-*b*-$PDEAEAM_{8k}$, $PNIPAM_{5k}$-*b*-$PDEAEAM_{5k}$ and $PNIPAM_{8k}$-*b*-$PDEAEAM_{2k.}$ Corresponding homopolymers PNIPAM and PDEAEAM with different molecular weights (2k, 5k, 8k and 10k) were also synthesized. The synthetic routes are illustrated in **Scheme 3**.

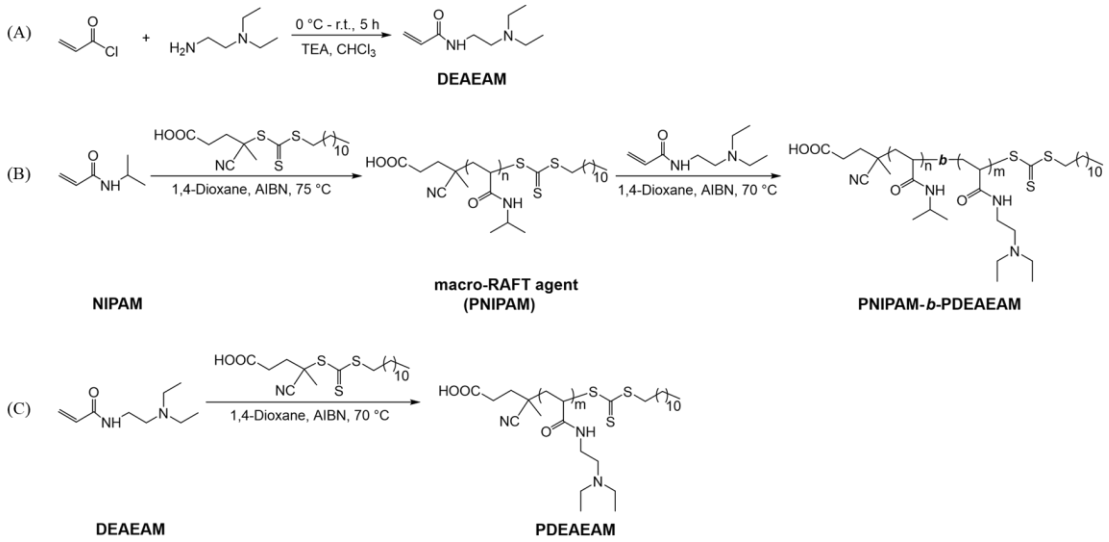

Scheme 3. Synthetic routes for (A) DEAEAM monomer, (B) PNIPAM-*b*-PDEAEAM copolymers (nk/mk values studied for the copolymer: 2k/8k, 5k/5k, 8k/2k) and (C) PDEAEAM homopolymer.

All PNIPAM, PDEAEAM and PNIPAM-*b*-PDEAEAM are abbreviated as PN, PD and PN-*b*-PD, respectively in the following.

The successful polymerization of DEAEAM from PN_{5k} macro-RAFT agent was assessed from ^{1}H NMR and FT-IR experiments, in which the spectrum of PN_{5k}-*b*-PD_{5k} shows both characteristic signals of PN_{5k} and PD_{5k} (**Figure 1** and **Figure S5**). The formation of copolymer was confirmed by diffusion-ordered spectroscopy (DOSY) experiments for which PN_{5k} and PN_{5k}-*b*-PD_{5k} present distinct and unique diffusion coefficient values at 2.8 and 2.4 × 10^{-10} $m^2 \cdot s^{-1}$ respectively (**Figure S6**).

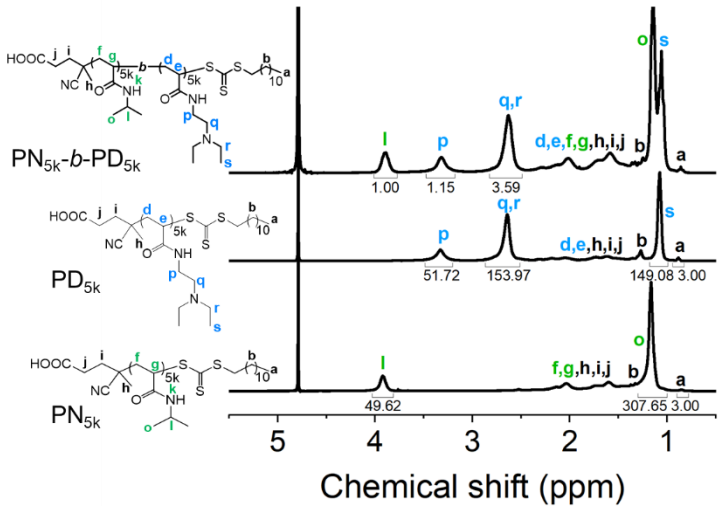

Figure 1. ^{1}H NMR spectra of PN_{5k} (bottom), PD_{5k} (middle) and PN_{5k}-*b*-PD_{5k} (top) in D_2O.

Average number molecular weights (M_n) and dispersity (Đ) were evaluated by size exclusion chromatography (SEC) in DMF or THF. PNIPAM macro-RAFT agents PN_{2k}, PN_{5k}, PN_{8k} and PN_{10k} were successfully obtained with well controlled molecular weight and dispersity e.g. below 1.09 (see **Table 1** and **Figure S7**). However, in the cases of PD homopolymers and PN-*b*-PD block copolymers the interaction between the nitrogen-containing polymer and SEC columns hampers the precise determination of molecular weights and induces the presence of a slight shoulder in DMF.[37] Nevertheless, as shown in **Figure 2,** a clear shift of the elution peak of PN_{5k}-*b*-PD_{5k} towards high molecular weight is evidenced compared to the one of macro-RAFT agent PN_{5k}. For rich PNIPAM copolymer PN_{8k}-*b*-PD_{2k} such a shift is only visible in THF (**Figures S8**). Molecular weights of copolymers were therefore calculated from ^{1}H NMR. For this, the integration value of peak **a** corresponding to methyl protons of dodecyl end group at 0.88 ppm were compared to signals of **l** and **p** protons at 3.92 and 3.33 ppm,

corresponding to PN (peak **l**) and PD (peak **p**), respectively (**Figures 1, S4 and S5** for PN_{5k}-*b*-PD_{5k}, PN_{2k}-*b*-PD_{8k} and PN_{8k}-*b*-PD_{2k} respectively). Detailed information on the characterization of synthesized diblock copolymers and their corresponding reference homopolymers are summarized in **Table 1**: a quite good agreement between theoretical molecular weights of (co)polymers and measured ones was found.

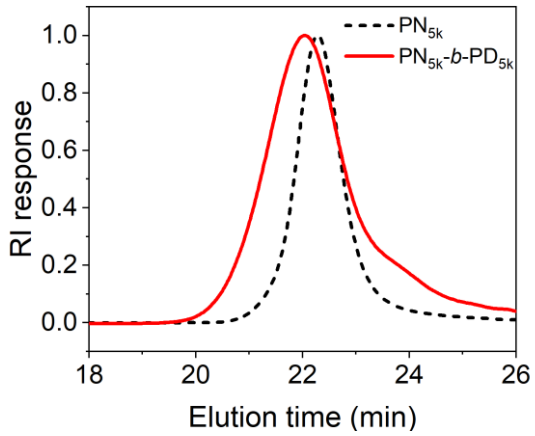

Figure 2. SEC chromatograms of PN_{5k} and PN_{5k}-*b*-PD_{5k} in DMF (containing 10 mM LiBr).

Glass transition temperatures (T_g) of diblock copolymers and their corresponding reference homopolymers were determined from DSC measurements **(Table 1)**. PN_{5k} and PD_{5k} homopolymers present a glass transition temperature at 104 and 30 °C respectively. Whereas in the case of PN_{5k}-*b*-PD_{5k}, only one intermediate transition was observed 55 °C. Moreover, whatever the composition, block copolymers present only one transition, which means PN and PD blocks have a good miscibility (**Figure S9**).

Table 1. Main characteristics of synthesized (co)polymers.

(co)polymer	DP_{PN}/DP_{PD} (theo.)	Conv. [a] (%)	T_g [b] (°C)	M_n			
				$M_{n,theo}$ [c] (g·mol^{-1})	$M_{n,NMR}$ (g·mol^{-1})	$M_{n,SEC}$ [d] (g·mol^{-1})	Đ[d]
PN_{2k}	14/0	97.0	86	1950	3940	2840 (1880)	1.02 (1.09)
PN_{5k}	41/0	99.9	104	5000	6130	6080 (4720)	1.06 (1.03)
PN_{8k}	67/0	99.6	116	7970	8880	9090 (7210)	1.07 (1.04)
PN_{10k}	84/0	98.9	129	9890	12280	12230 (10010)	1.09 (1.04)
PN_{2k}-*b*-PD_{8k}	14/43	90.8	52	9290	12580	9860 (8940)	1.32 (1.14)
PN_{5k}-*b*-PD_{5k}	41/28	96.6	55	9840	11090	8340 (6860)	1.09 (1.16)
PN_{8k}-*b*-PD_{2k}	67/9	78.5	72	9480	10220	10720 (9120)	1.08 (1.01)
PD_{2k}	0/10	99.8	31	2000	2160	(2500)	(1.06)
PD_{5k}	0/26	95.4	30	4790	4810	6900 (4210)	1.21 (1.09)
PD_{8k}	0/40	96.0	35	7290	8830	7820 (7210)	1.63 (1.41)
PD_{10k}	0/52	93.5	25	9350	9080	10740 (7730)	1.37 (1.19)

[a] Conversion determined by ^{1}H NMR spectra; [b] T_g measured by DSC with a heating rate of 10 °C·min^{-1}; [c] $M_{n,theo} = ([M]_0 \times M_n(M))/[RAFT]_0 \times (Conv.\%) + M_n(RAFT)$; [d] $M_{n,SEC}$ and Đ determined by SEC analysis in DMF containing 10 mM LiBr (in THF containing 2 vol.% TEA).

3.2. pH- and thermo-responsive behavior of PN and PD homopolymers.

To understand the thermoresponsiveness of PN-*b*-PD under different conditions of pH and temperature, the behavior of PN and PD homopolymers was firstly investigated.

a. PN homopolymer.

PNIPAM is by far the most commonly described thermoresponsive polymer. Incorporation of hydrophilic or hydrophobic comonomers enables to finely tune cloud point temperature (T_c).[1,38] For example, when NIPAM is statistically copolymerized with hydrophilic monomers such as acrylamide, T_c increases up to about 45 °C when the polymer chain comprises 18 mol.% of acrylamide, whereas T_c decreases to about 26 °C when 20 mol.% of less hydrophilic acrolein is incorporated into the polymer chain.[1] To a lesser degree, similar effects are observed for polymer presenting different architectures like block or branched copolymers.[1,39-43] Interestingly terminal groups can also have a strong influence: whereas hydrophobic terminal groups decrease T_c, hydrophilic ones have a reverse effect.[44] Here, synthesized PN_{xk} bears, at pH 4, one hydrophilic carboxylic acid function on one side and a hydrophobic $-C_{12}H_{25}$ group on the other side (**Scheme 4**). Their presence might therefore hamper the thermoresponsiveness of PN_{xk} homopolymers in aqueous solution.

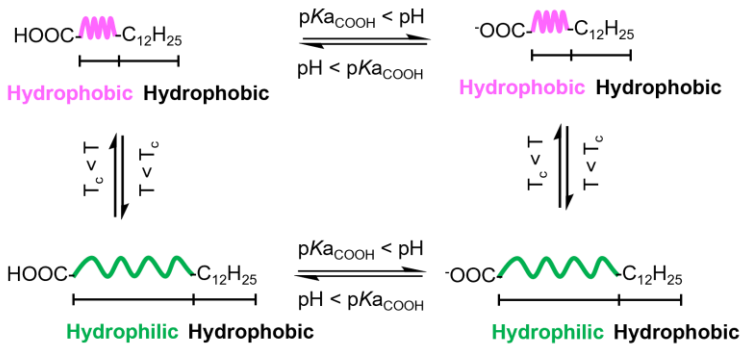

Scheme 4. Structure and effect of temperature on the conformation of PN chains.

At pH 4, T_c measurement of 1 wt.% PN homopolymer solution by DLS, turbidity and DSC analyses shows a non-linear increase of T_c from 16 to 29 °C when molecular weight increases from 2000 g·mol^{-1} to 10000 g·mol^{-1} (**Figure S10)**. The observed tendency is mainly ascribed to the nature of terminal group. The presence of a hydrophobic -$C_{12}H_{25}$ tail group tends to weaken the solvation of homopolymer in water, resulting in a significant decrease of measured T_c. This effect is as expected more pronounced for polymers with low molecular weight.[45] Polymer concentration also has a drastic effect: for PN_{5k} with a concentration of 1 wt.%, T_c was measured at 28 °C and this value increases to 32 °C as concentration drops to 0.5 wt.% (either by DLS or transmittance measurement). Indeed, interactions between polymer chains promotes the formation of large aggregates at higher concentration (**Figures S11 and S12**). As stated above, one extremity of the polymer bears a carboxylic function with a p*K*a value around 4.5. Thus, a change in T_c of synthesized PN is expected upon a modification of pH, which leads to the change in ionization/hydration state of end group. The thermoresponsive character of PN_{5k} at different pH values was studied by turbidity measurements as depicted in **Figure 3A**.

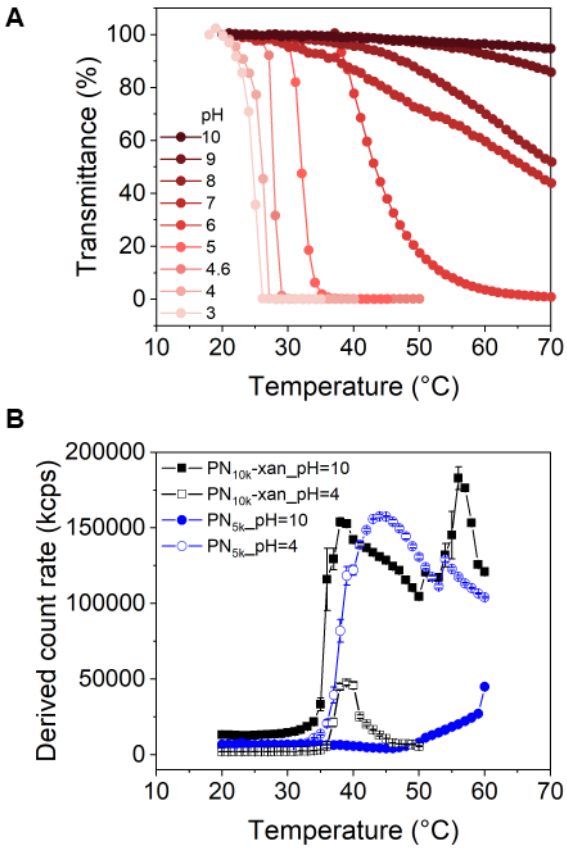

Figure 3. A. Transmittance change of PN_{5k} versus temperature at different pH values ($[PN_{5k}]$ = 1 wt.%, heating rate: 1 °C·min^{-1}). B. Derived count rate as a function of temperature for PN_{10k}-xanthate and for PN_{5k} at pH 4 and 10, respectively ([PN] = 0.1 wt.%). NB: beyond the transition temperatures, derived count rate measurements are impacted by aggregation/settling phenomena which in some cases lead to decreases in the measured intensity.

PN_{5k} displays a clear LCST behavior within a pH range from 3 to 6 with corresponding T_c value increasing from 25.1 to 40.1 °C. For pH value higher than 6, the transmittance at 70 °C no longer declines to 0 with measured values at 44, 52 and 86% at pH 7, 8 and 9 respectively and no detectable decrease in transmittance was observed at pH 10. In

order to confirm the critical role of end group in the observed behavior, a PN homopolymer was synthesized by using 2-mercaptopropionic acid methyl ester *O*-ethyl dithiocarbonate (Rhodixan A1) RAFT agent.[43,34] As expected, no significant pH-dependance of thermo-responsive behavior is observed for this homopolymer (**Figure S13**). The pH-dependence of T_c can be attributed to the degree of ionization of -COOH end group. Compared to -COOH group, $-COO^-$ has a better solvation and helps to improve PN_{5k} solubility in water. With rising pH, the amount of $-COO^-$ groups in solution becomes larger and results in an increase of T_c. Such trend was previously reported in the cases of linear and star-typed PN homopolymers terminated with -COOH or ionizable groups (pKa_{COOH} = 4.07 ± 0.1).[36,44,46] In addition, the absence of transition observed at high pH value can be ascribed to the formation of micellar system which hinders phase separation. Such a behavior was previously reported in literature for PN homopolymers synthesized by RAFT polymerization using S-1-dodecyl-S-(α,α'-dimethyl-α,α'-acetic acid) trithiocarbonate as chain transfer agent: this polymer chains form micelles in aqueous solutions with a core of hydrophobic terminal dodecyl groups and a corona of PN chains with carboxylic groups at the periphery, the ionization of which prevents phase separation of PN at temperature above T_c.[44] In order to confirm here the formation of micellar system and the critical role of end group, DLS measurements were performed as a function of temperature at two different pH values (4 and 10) and the behavior of PN_{5k} was compared to that of PN_{10k}-xanthate (without carboxylic acid end-group and long alkyl chain). At pH 4, whatever the nature of end groups both homopolymers present clear transitions with the formation of aggregates

larger than 250 nm when temperature increased to 60 °C (**Figure 3B**). As expected from partial protonation of carboxylate functions, zeta potential values around -10 mV are found for PN_{5k} (**Figure S15**): this lower zeta potential does not enable to obtain stable colloidal structures and favored aggregation process upon heating as illustrated in **Scheme 5**. At pH 10, the xanthate terminated PNIPAM with a concentration of 1 wt.% presents a transition at 35 °C that induces the formation of large aggregates (size around 500 nm). PN_{5k} displays a completely different behavior. Indeed, it forms poorly defined nanoobjects in a low temperature range (20 – 32 °C), and forms small defined objects with an average diameter around 15 nm as temperature rises to 33 °C (above T_c) (**Figure 3B and Figure S14**). Moreover, whatever the temperature (below or above T_c), a highly negative zeta potential was measured around –45 mV (**Figure S15**) which is in agreement with nanoobjects bearing carboxylate functions as an outer shell. These measurements suggest the formation of micelles stabilized by negatively charged carboxylate functions since increasing temperature results in contraction of PNIPAM chains as illustrated in **Scheme 5**.

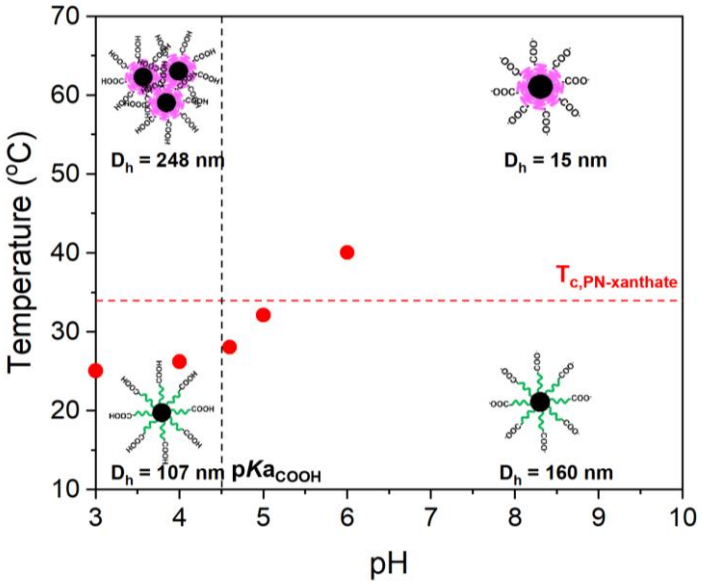

Scheme 5. Schematic phase diagram of PN_{5k} in aqueous solution as a function of pH and temperature (1 and 0.1 wt.% of PN_{5k} used for cloud point and hydrodynamic diameter determinations).

b. PD homopolymers.

PD homopolymer is a weak polyelectrolyte, fully soluble in water whatever the pH at low temperature. The p*K*a value of pendant tertiary amino groups was determined by pH-titration curve (**Figure S16**) and a value of 7.25 was detected. This value is significantly lower than the one measured for the corresponding monomer at 9.17 and is close to the p*K*a values measured for PDEAEMA and PDMAEMA at 7.5 and 7.4 respectively.[47] At pH below 7.25, PD is fully protonated, increasing pH reduces the number of positive charges among PD chains. Transmittance of aqueous solution of PD_{5k} at different pH values was then measured as a function of temperature (**Figure 4**).

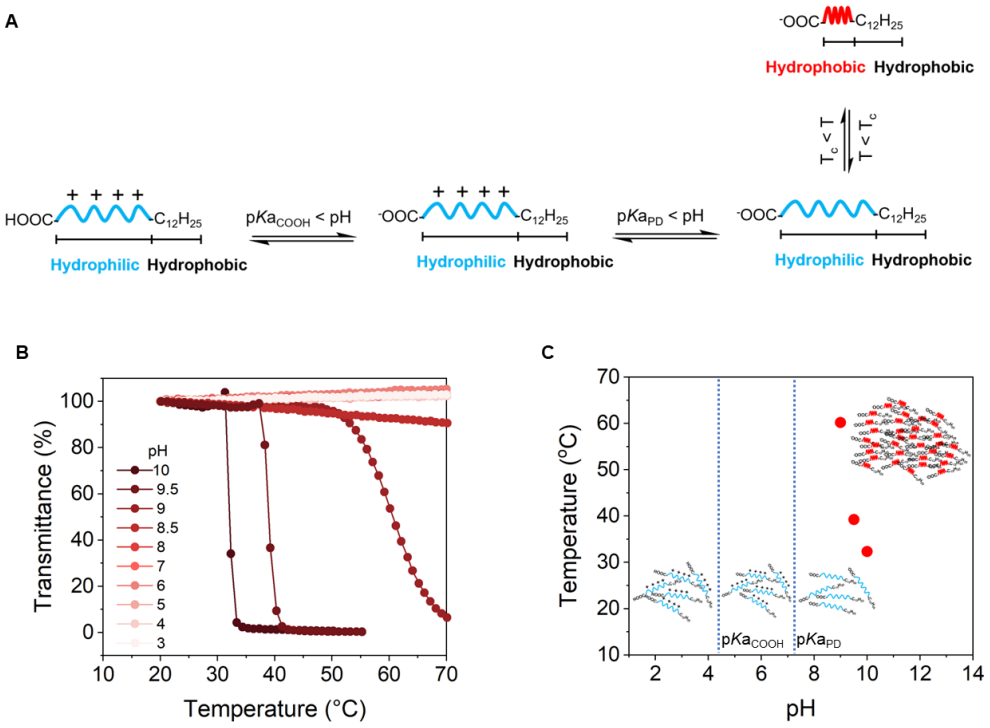

Figure 4. A. Effect of temperature and pH on the structure of PD chains. B. Transmittance change of PD_{5k} as a function of temperature at different pH values ([PD_{5k}] = 1 wt.%). C. Schematic illustration of thermoresponsiveness and self-assembly behavior of PD_{5k} solution at different pH values.

For a pH value below 8, no transmittance change was detected between 20 and 70 °C. At higher pH value, a T_c value was measured which drops sharply from 60.2 °C at pH 9 to 32.3 °C at pH 10. Above p*Ka*$_{PD}$, the deprotonation of diethylamino group limits the solubility of PD_{5k} chain at high temperature and induces a LCST behavior with a measured T_c correlated with the level of protonation of polymer chains. Upon heating large aggregates around 160 - 300 nm with positive zeta potential are formed and results in cloudy solution (**Figure S17**). In addition, the effect of molecular weight and polymer concentration on thermoresponsive properties were then studied at pH 10

(above pKa$_{PD}$). It is observed that increasing molecular weight from 2000 to 10000 g·mol^{-1} shifts T_c from 31.07 to 41.02 °C. (**Figure S18**). Moreover, an increase of concentration of PD_{5k} aqueous solution from 0.1 to 0.5 wt.% leads to a decrease of T_c from 37.1 to 32.3 °C with no further variation when concentration increases up to 1 wt.% (**Figure S19**). This trend is similar to the one observed in the case of PN_{5k} described in previous section and is related to the interactions between polymer chains, which promotes the formation of large aggregates at higher concentration. It has to be noted that contrary to what observed for PN_{5k} the formation of well-defined structures induced by the effect of chain end was not detected in the case of PD_{5k}. At pH below pKa$_{PD}$, aggregates with hydrodynamic diameter around 50 nm were measured from DLS experiments. These aggregates have a positive zeta potential (around 25 mV) as expected from the protonated form of diethylamino groups. Heating PD_{5k} solution to 60 °C tends to slightly increase the size of these aggregates (up to 100 nm) that remains positively charged, which keeps the aqueous solution transparent.

3.3. Thermoresponsive behavior of PN-*b*-PD solution.

PN-*b*-PD block copolymers comprises two stimuli responsive blocks: a thermoresponsive PN block with a characteristic transition temperature at 30 °C (at 1 wt.%) and a PD block which is, at pH higher than pKa$_{PD}$ (i.e. 7.25), deprotonated and thermoresponsive. In addition, two end groups (-COOH and -$C_{12}H_{25}$ group) are prone to promote the formation of micellar system above pKa$_{COOH}$ as demonstrated in the case of PN_{5k}. The behavior of PN_{5k}-*b*-PD_{5k} block copolymer in aqueous solution was then

studied at different pH by means of scattering, microscopy and NMR measurements. The colloidal properties are illustrated in the following in the case of PN_{5k}-*b*-PD_{5k}.

a. Thermoresponsive behavior of PN_{5k}-*b*-PD_{5k} at pH above p*Ka*$_{PD}$.

At pH value above p*Ka*$_{PD}$ (i.e 7.25), PN_{5k}-*b*-PD_{5k} comprises two thermoresponsive blocks, PD and PN, a -COOH end group in its carboxylate anionic form ($-COO^-$) and a hydrophobic $-C_{12}H_{25}$ end group (**Scheme 6**).

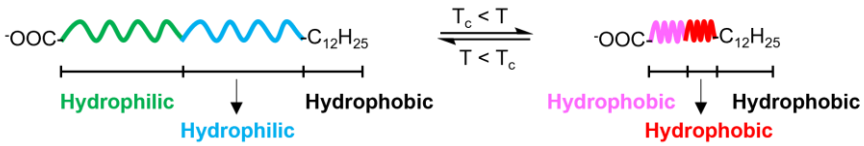

Scheme 6. Structure and effect of temperature on the conformation of PN-*b*-PD chains at pH 10 above p*Ka*$_{PD}$.

Surface tension of PN_{5k}-*b*-PD_{5k} solutions was measured at 20 °C as a function of concentration (**Figure 5A**). The adsorption of block copolymer to water-air interface results in a decrease of surface tension up to a critical aggregation concentration (CAC) equal to 3×10^{-3} wt.%. Nevertheless, a further slower decrease of surface tension is still observed after the CAC value that might be relative to a slow reorganization of the polymer at the interface or in solution. The solubility of PN_{5k}-*b*-PD_{5k} at pH 10 was investigated by turbidimetry, DLS and ^{1}H NMR experiments above apparent measured CAC. For a concentration equal to 1 wt.%, whereas, upon heating, PN_{5k} solution showed no significant change in transmittance due to the formation of micelles, both PD_{5k} and PN_{5k}-*b*-PD_{5k} solutions undergo a transparent-to-cloudy transition at 34 °C and

38 °C respectively (**Figure 5B**), large assemblies are formed by aggregation of PN_{5k}-*b*-PD_{5k} chains at temperature above T_c as evidenced by DLS results **(Figure 5C)**.

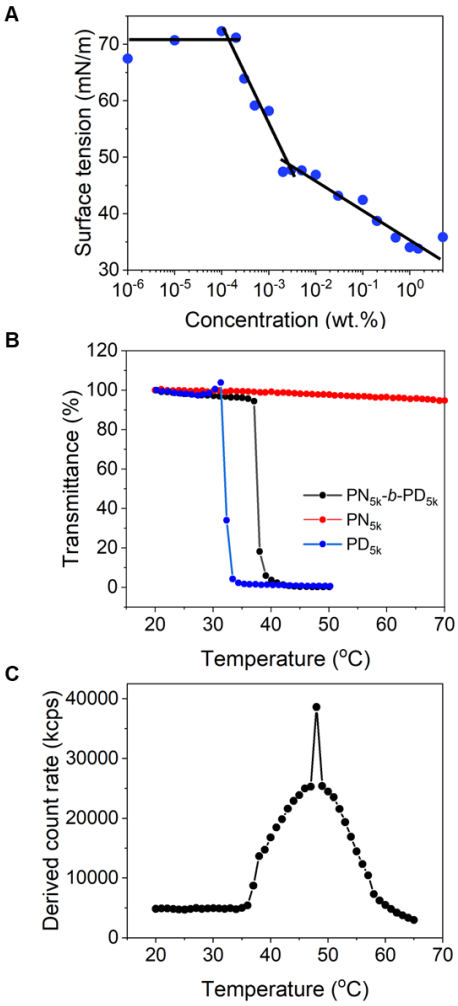

Figure 5. A. Evolution of surface tension of PN_{5k}-*b*-PD_{5k} solution at pH 10 as a function of concentration at 20 °C. B. Plots of transmittance versus temperature of PN_{5k}-*b*-PD_{5k}, PN_{5k} and PD_{5k} at pH 10 ([(co)polymer] = 1 wt.%; heating rate 1°C·min^{-1}). C. Derived count rate obtained from DLS measurements of PN_{5k}-*b*-PD_{5k} solution at 0.1 wt.% as a function of temperature at pH 10 (NB: after 50°C the observed decreased is induced by an aggregation phenomenon). T_c values of PN_{5k}-*b*-PD_{5k} determined by different techniques at pH 10 are given in **Table S2**.

In order to have a further understanding of the mechanism behind this transition, ^{1}H NMR analysis was performed in temperature range of 20 - 50 °C (**Figure 6A**).

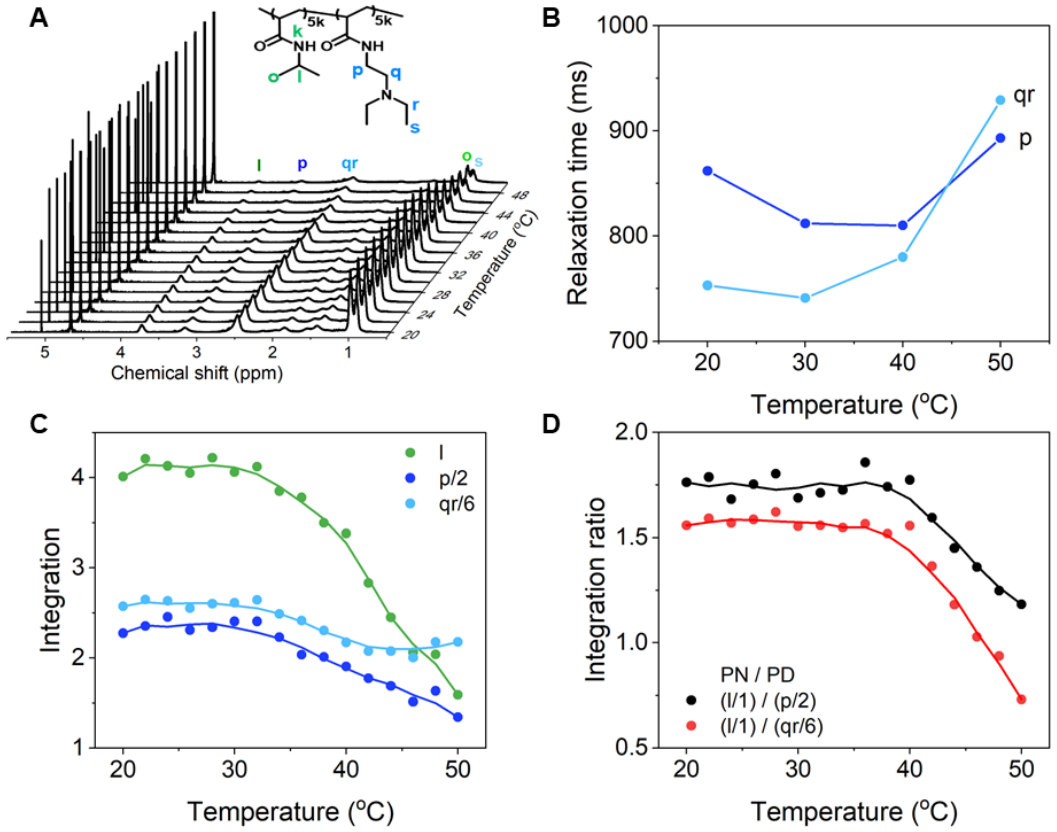

Figure 6. A. ^{1}H NMR spectra of PN_{5k}-*b*-PD_{5k} as a function of temperature at pH 10 (trioxane as internal standard with a chemical shift at 5.1 ppm and integral of 1 at whatever temperature studied). B. Evolution of relaxation time (T_1) of different protons as a function of temperature. C. Evolution of integration of characteristic peaks in PN_{5k}-*b*-PD_{5k} relatively to the reference peak of trioxane. D. Evolution of integration ratio between PN and PD block as a function of temperature. ([PN_{5k}-*b*-PD_{5k}] = 1 wt.%, in D_2O)

Figure 6B illustrates the evolution of longitudinal relaxation time (T_1) as a function of temperature. At 20 °C, all measured T_1 values are above 750 ms, indicating the formation of aggregates, probably through the hydrogen bonds formed among polymer chains in solution. When temperature approaches to 40 °C, T_1 value corresponding to the protons in α position of amide function in PN units (**l**) rapidly reaches 1600 ms. This might be ascribed to the restricted motion of polymer chains consecutive to a dehydration phenomenon. Meanwhile, T_1 values corresponding to characteristic protons of PD block (**p**, **q** and **r**) do not increase to such an extent. It appears that the dehydration mainly affects the mobility of PN block and that PD chains present a higher mobility in aqueous solution. This hypothesis is further confirmed by the evolution of integrals of characteristic protons associated to PD (2.5 and 3.2 ppm) and PN (3.8 ppm) units as a function of temperature. As depicted in **Figure 6C**, the integral corresponding to PN and PD units remains roughly constant up to 32 °C. Subsequently, both signals of PD and PN decreases slowly but their integral ratio remains constant (**Figure 6D**) with increasing temperature due to a progressive dehydration phenomenon of both blocks. As temperature rises to 38 °C, a pronounced decrease is only observed for the signal relative to PN and results as depicted in **Figure 6D** to a decrease of the integral ratio. These discrepancies observed between PN and PD blocks at 38 °C comfort the formation of aggregates where PN chains are in a more pronounced dehydrated state than PD chains.

The aggregates obtained from aqueous solution of PN_{5k}-*b*-PD_{5k} below and above T_c were characterized by TEM, FF-TEM, DLS and SAXS techniques. At 25 °C (below

T_c), TEM images reveal the presence of small spherical aggregates with an average diameter equal to 23 ± 6 nm, which is in good accordance with what found from DLS measurement (a hydrodynamic diameter 27 ± 9 nm and a negative zeta potential –3 ± 2 mV at pH 10 and –28 ± 4 mV at pH 11). This self-assembly behavior in PN-*b*-PD is caused by the hydrophobic terminal group (-$C_{12}H_{25}$) as well as the hydrophilic PN and PD segments. In the literature, micelles with 10 - 20 nm hydrodynamic radius are reported for polymers with similar molecular weight and structure.[48,49] These self-assemblies are described as hairy micelles with small core of few nm radius.[44,48] This corresponds well to SAXS results (**Figure 7**). The SAXS curves of PN_{5k}-*b*-PD_{5k} solution present a power law dependence on the scattering vector in the Porod region indicative of swollen chains in good solvent ($I(q) \sim q^{-\alpha}$, with $\alpha = 1.6$). From the Guinier region a radius of gyration (R_g), 3.5 ± 1 nm is evaluated, which corresponds to the core of hairy micelles. Besides, a model for star polymer could be used to describe the data and an aggregation number of 1.5 was obtained, indicating the possible presence of both small micelles and free polymer chains.

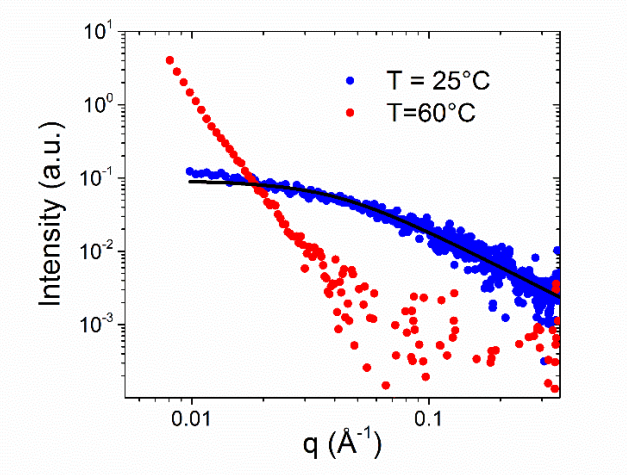

Figure 7. SAXS curves of PN_{5k}-*b*-PD_{5k} solution at 25 and 60 °C ([PN_{5k}-*b*-PD_{5k}] = 1 wt.%, pH = 10).

At 60 °C (above T_c), the SAXS profile completely changes and large structures with size outside the experimental accessible range are formed. Indeed, no Guinier region but an extended Porod region with a slope of –4 is observed, indicating the aggregates are quite compact in accordance with ^{1}H NMR results showing the collapse of PN and PD chains. The morphology of PN_{5k}-*b*-PD_{5k} was further investigated by TEM and FF-TEM techniques, spherical objects with diameter of 93 ± 35 and 174 ± 76 nm are observed, respectively (**Figure 8B, D** and **F**). Negative zeta potential values were measured and found slightly below the values measured at 25 °C (–5 ± 2 mV at pH 10 and –35 ± 4 mV at pH 11), carboxylate function present at the surface of nanoobjects might be responsible for that.

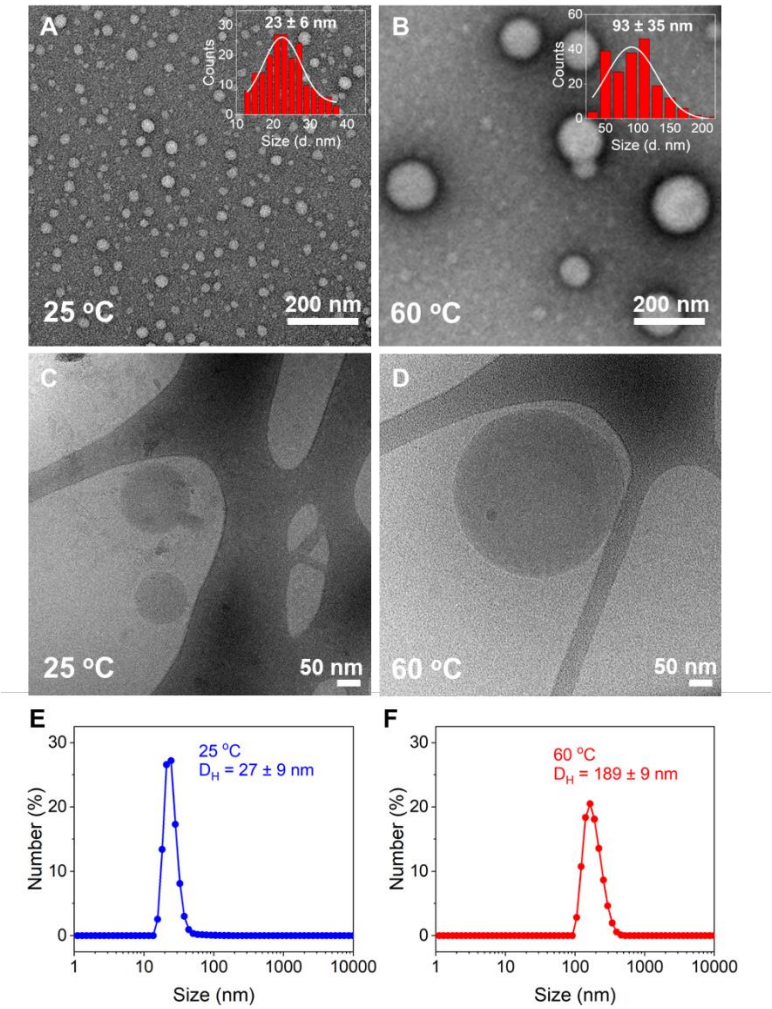

Figure 8. TEM, FF-TEM images and Number-averaged size distribution of PN_{5k}-*b*-PD_{5k} at 25 °C (A, C, E) and at 60 °C (B, D, F) at pH = 10. TEM samples were stained with 2 wt.% uranyl acetate solution.

To gain a further understanding of the underlying aggregation mechanism and of its kinetic, turbidimetry experiments were performed at different heating rates. As illustrated in **Figure 9A**, whereas at a heating rate equal to 0.2 °C·min^{-1}, T_c is measured at 35 °C, this value rises to 40 °C for a heating rate equal to 5 °C·min^{-1}. Moreover, it has to be noted that measured hydrodynamic diameters depend dramatically on the history of measurements. Hence keeping one sample at 60 °C over a period of 2 h

induced a progressive increase of measured hydrodynamic diameters from 130 to 180 nm as shown in **Figure 9B**. Lastly, a sample was heated from 20 to 65 °C by step of 5 °C staying 10 min at the targeted temperature and by cooling down the sample to 20 °C before performing the next heating step (**Figure 9C**). Measured hydrodynamic diameters (Number-distributed) are found around 250 nm above T_c (i.e above the values measured in the previous experiment depicted in Figure 9B) and around 20 nm below T_c. Therefore, measured size above T_c but also at 20 °C depends on the history of measurements.

These different experiments illustrate the key role of polymer history in the reorganization of polymer/colloidal structure within the aggregates. This reorganization occurs with characteristic timescale within minutes to hours. Moreover, the measured size of aggregates depends strongly on experimental process (heating rate, equilibrating time, kinetic…) and a possible reorganization of polymer/colloidal structure occurred within the aggregates. Noteworthy, polymer concentration is another parameter to be considered to have a precise control over the size of formed aggregates.

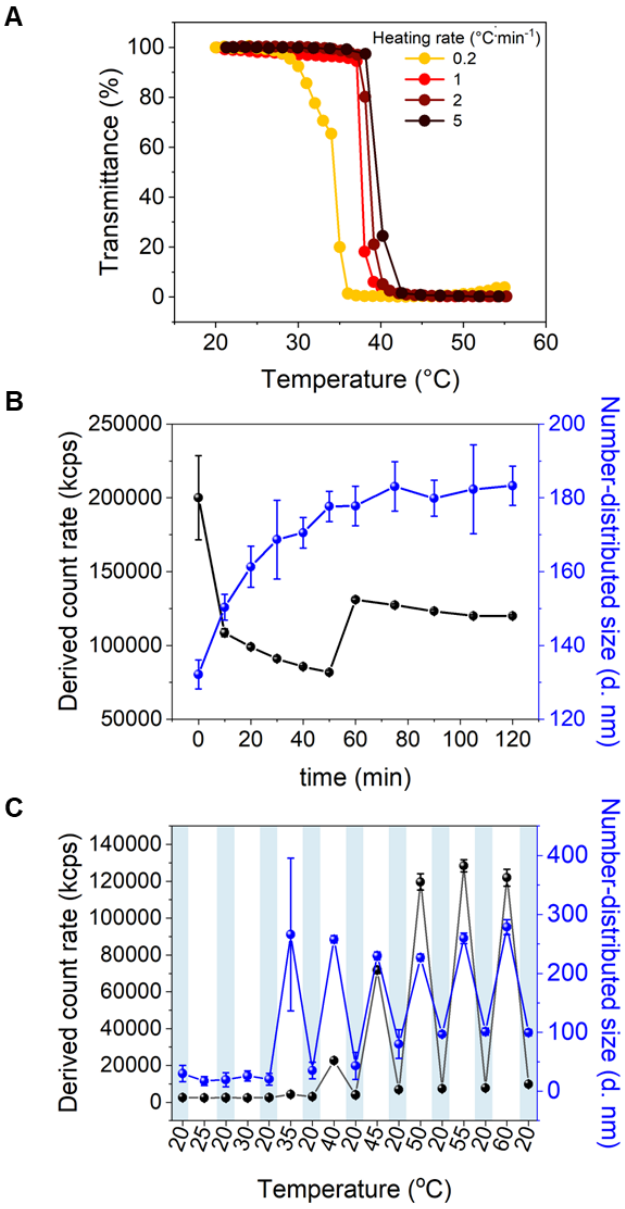

Figure 9. A. Transmittance change of PN_{5k}-*b*-PD_{5k} versus temperature at pH 10 with different heating rates ([PN_{5k}-*b*-PD_{5k}] =1 wt.%). B. Derived count rate and Number-distributed size change of PN_{5k}-*b*-PD_{5k} aggregates versus time at 60 °C (pH = 10, [PN_{5k}-*b*-PD_{5k}] = 0.1 wt.%). C. Evolution of Derived count rate and Number-distributed hydrodynamic diameter when performing experiments in which a copolymer solution (0.1 wt.%) was heated and kept for 10 min at the chosen temperature then cooled down at 20 °C before performing another heating process at another temperature.

To conclude on the behavior of PN_{5k}-*b*-PD_{5k} at high pH value, experimental measurements suggest that free polymer and pre-existing aggregates which are also present at 25 °C tend to aggregate upon heating. The presence of carboxylate function might explain the observed limitation of aggregation process. As stated above, the extent of aggregation depends strongly on the kinetic consideration and the history of colloid preparation. Moreover, NMR results demonstrate that PN chains upon dehydration are present in more constrained environment than PD chains. Based on these analyses, the morphologies of PN_{5k}-*b*-PD_{5k} aggregates below and above T_c at pH 10 are proposed in **Scheme 7**.

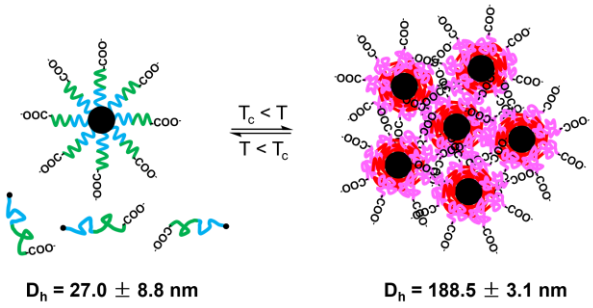

Scheme 7. Schematic illustration of self-assembly structures of PD_{5k}-*b*-PD_{5k} solution below and above T_c at pH 10.

b. Thermoresponsive behavior of PN_{5k}-*b*-PD_{5k} at pH below p*Ka*$_{PD}$.

At pH 4, PN_{5k}-*b*-PD_{5k} comprises one thermoresponsive groups (PN), one cationic hydrophilic block (PD), a -COOH end group and a hydrophobic -$C_{12}H_{25}$ end group (**Scheme 8**).

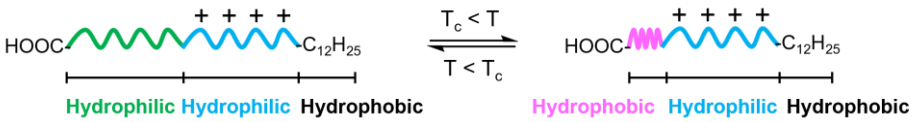

Scheme 8. Structure and effect of temperature on the conformation of PN-*b*-PD chains at pH 4.

With a profile similar to the one observed at pH 10, a CAC equal to 2×10^{-3} wt.% can be evaluated from the surface tension measurements performed at 20 °C (**Figure S20**) which is roughly similar to the one found at pH above pKa (3×10^{-3} wt.%, **Figure 5**). Protonation of PD units does not modify significantly the adsorption of the polymer at interfaces. The effect of temperature on the solubility behavior at pH 4 was assessed by DLS, turbidimetry and ^{1}H NMR experiments above measured CAC. Visually, colloidal solutions undergo a transition from transparent to cloudy solutions around 28 °C and the formation of large aggregates was evidenced by DLS measurements (**Figure 10A**). Interestingly, the increase of the signal seems to take place in two steps. After the first increase at 26 °C, a second transition seems to occur at 36 °C after which the measured diameter still increases (more than 1000 nm), whereas derived count rate strongly decreases due to a partial decantation of formed aggregates. The evolution of transmittance as a function of temperature for PN_{5k}-*b*-PD_{5k}, PN_{5k} and PD_{5k} at pH 4 is

shown in **Figure 10B**. Whereas PN_{5k} homopolymer has a T_c at 26.2 °C, no transmittance change of PD_{5k} takes place in the studied temperature range. Indeed, PD_{5k} is protonated and no more thermoresponsive. In the case of PN_{5k}-*b*-PD_{5k}, a two-step transmittance decrease occurred starting at 23 °C with a first inflection point at 29 °C ($T_{c,1}$) and a second one at 39 °C ($T_{c,2}$). The first transition at 29 °C might come from the thermoresponsive character of PN segment. Above $T_{c,1}$, PN chains in PN_{5k}-*b*-PD_{5k} collapse, inducing a reorganization of the colloidal structures formed at room temperature. With the increase of temperature, zeta potential was also measured with an increasing tendency (**Figure 10C**), which is in good agreement with a reorganization to form objects with a PN dehydrated core and a shell of PD block in positively charged form.

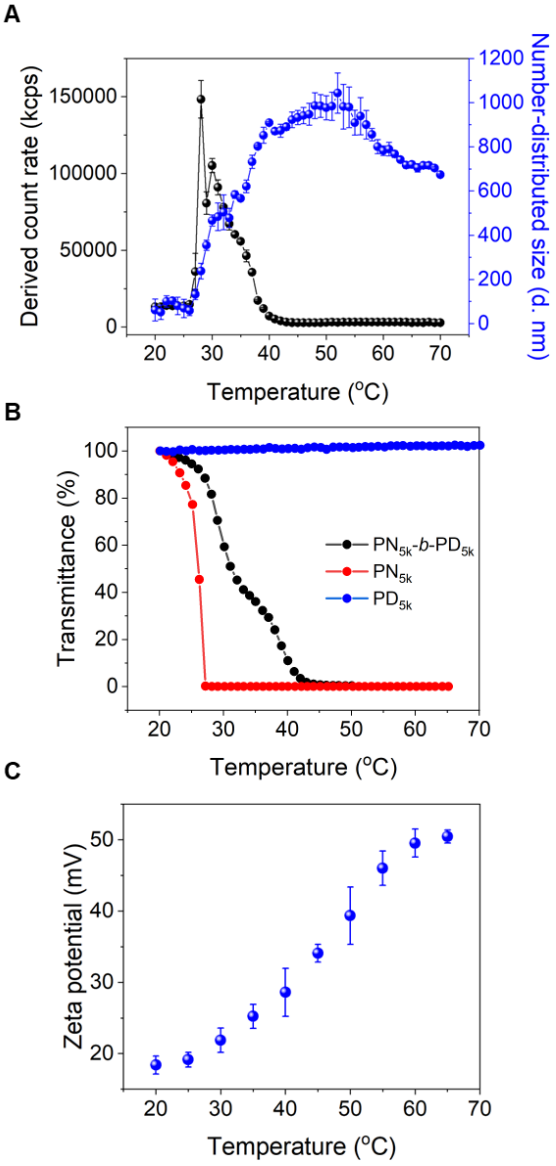

Figure 10. A. Evolution of Derived count rate and Number-distributed size distribution of PN_{5k}-*b*-PD_{5k} as a function of temperature ([PN_{5k}-*b*-PD_{5k}] = 1 wt.%, pH = 4). B. Transmittance change of PN_{5k}-*b*-PD_{5k}, PN_{5k} and PD_{5k} at pH 4 as a function of temperature ([(co)polymer] = 1 wt.%, heating rate = 1 $^{o}C \cdot min^{-1}$). C. Evolution of Zeta potential of PN_{5k}-*b*-PD_{5k} at pH 4 as a function of temperature.

When temperature raises up to $T_{c,2}$ (39 °C), these colloids undergo the second transition with the formation of aggregates with a poor colloidal stability. In order to have a deep understanding of the mechanism behind these transitions, ^{1}H NMR analyses were performed using trioxane as reference compound upon heating from 20 to 50 °C (**Figure 11A**). **Figure 11B** illustrates the evolution of relaxation time (T_1) as a function of temperature.

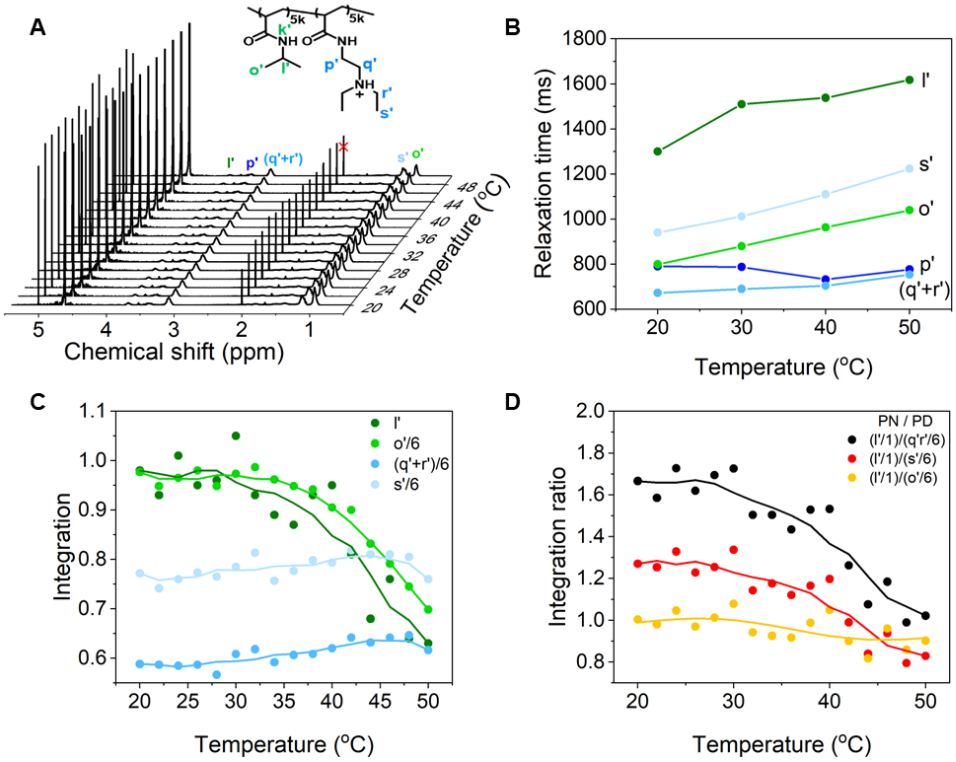

Figure 11. A. ^{1}H NMR spectra of PN_{5k}-*b*-PD_{5k} as a function of temperature at pH 4 (trioxane as internal standard with a chemical shift at 5.1 ppm and integral of 1 at whatever temperature studied). B. Evolution of relaxation time (T_1) of characteristic peaks in PN_{5k}-*b*-PD_{5k} as a function of temperature. C. Evolution of integration of characteristic peaks in PN_{5k}-*b*-PD_{5k} relatively to the reference peak of trioxane. D. Evolution of integration ratio between PN and PD block as a function of temperature.

At 20 °C, all measured T_1 values are above 600 ms, evidencing the formation of colloids. When temperature increases up to 50 °C, measured relation times T_1 for protons corresponding to PN segment increases. Restricted motion of polymer chains consecutive to a dehydration phenomenon and formation of larger objects might be responsible for this observation. At the same time, T_1 of protons corresponding to PD block does not increase to such an extent. The increase of temperature seems to affect mainly PN block. These T_1 values were further considered to acquire ^{1}H NMR spectra in quantitative conditions and to determine the evolution of the integration of protons associated to PD and PN units relatively to the integral of trioxane. As depicted in **Figure 11C**, while the integration area of PD signals remained roughly constant, the ones corresponding to PN starts to decrease at 30 °C, this result is also showed in **Figure 11D** by the decreasing tendency of integral ratio between PN and PD blocks upon heating. These discrepancies observed between PN and PD blocks at 30 °C comfort the formation of aggregates from preexisting colloids induced by the dehydration upon heating of PN block while PD remains locally hydrated.

The colloidal assemblies present in PN_{5k}-*b*-PD_{5k} aqueous solution were studied by TEM, DLS at 25 (below $T_{c,1}$), 30 (between $T_{c,1}$ and $T_{c,2}$) and 60 °C (above $T_{c,2}$). All results are summarized in **Table 2.** To avoid aggregation phenomenon observed at 1 wt.%, solutions with a concentration of 0.1 wt.% were studied. Number-averaged hydrodynamic diameters are 26, 77 and 200 nm measured at 25 °C ($T < T_{c,1}$), 30 °C ($T_{c,1} < T < T_{c,2}$) and 60 °C ($T > T_{c,2}$) (**Table 2** and **Figure 12F**), respectively. At 25 °C,

TEM image shows the presence of small spherical aggregates with an average diameter of 23 ± 5 nm (**Figure 12A**). Moreover, some large aggregates with hydrodynamic diameter between 20 to 100 nm can be only evidenced by DLS measurement and might be present in solution in small amounts. The interactions between protonated PD and PN might be at the origin of these aggregates. At 30 °C (above $T_{c,1}$), PN chains start to collapse due to the dehydration phenomenon confirmed by NMR experiments.

Table 2. PN_{5k}-*b*-PD_{5k} aggregates size at different temperatures determined by TEM, DLS and FF-TEM measurements.

pH	T (°C)	TEM (d. nm)	DLS (d. nm)[a]	FF-TEM (d. nm)[b]
4	25	23 + 5	26 + 9	31 + 12
	30	30 ± 9	77 ± 9	/[c]
	60	126 ± 39	200 ± 5	160 ± 74

[a] Obtained from number-averaged size distribution; [b] Measured at 50 °C; [c] Not determined. (PN_{5k}-*b*-PD_{5k} concentrations of 0.1, 0.1 and 0.5 wt.% for TEM, DLS and FF-TEM measurements, respectively).

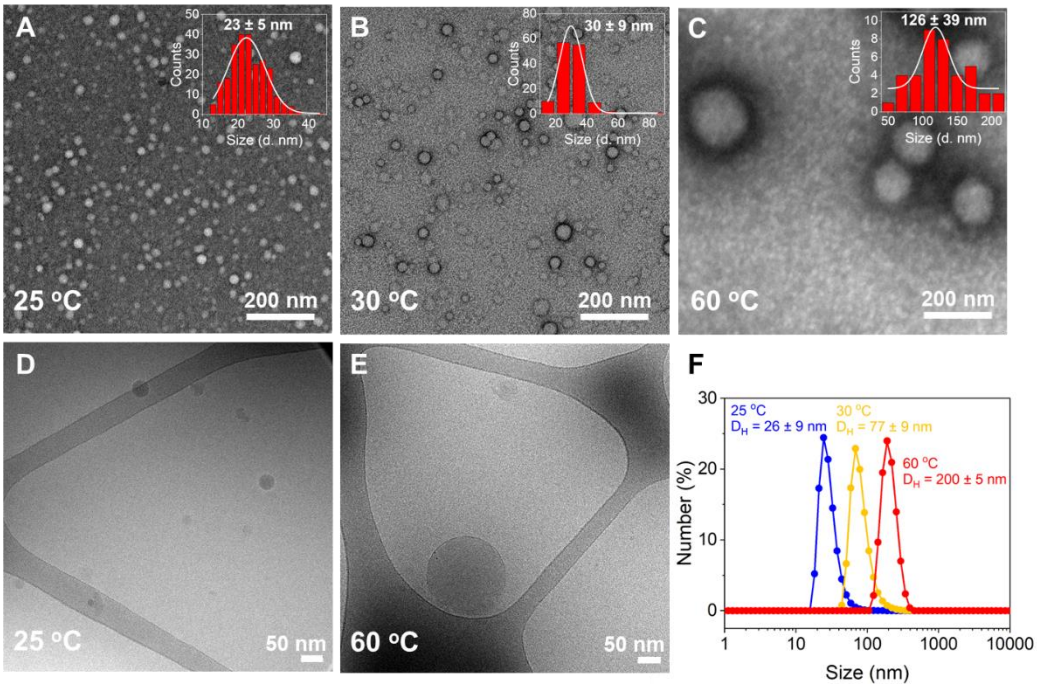

Figure 12. TEM, FF-TEM images at 25 (A,D), 30 (B) and 60°C (C, E). F. Number-averaged size distribution of aggregates for PN_{5k}-*b*-PD_{5k} formed at pH 4 (TEM samples were stained with 2 wt.% uranyl acetate solution, PN_{5k}-*b*-PD_{5k} concentration for TEM and DLS measurements was 0.1 wt.%, for FF-TEM analysis was 0.5 wt.%).

However, PD still maintains cationic character and exhibits hydrophilic property in water. As suggested from TEM images (**Figure 12B**), PN_{5k}-*b*-PD_{5k} assembles into flower-like micelles with a diameter equal to 30 ± 9 nm. These structures can be issued from a rearrangement of polymer chains in a core shell structure with hydrophobic -$C_{12}H_{25}$ end group in the core and PN partially dehydrated block and hydrated cationic PD segment in the shell interacting together and were previously observed by other authors.[43] When temperature goes higher than $T_{c,2}$, larger spherical aggregates are formed (**Figure 12C** and **E**, diameter equal to 126 ± 39 nm and 160 ± 74 nm by TEM

and FF-TEM, respectively) in good accordance with DLS results. These structures could result from aggregation of previous ones or/and a more pronounced phase separation between PN and PD blocks.

In order to get some insight in the morphologies of these assemblies, SAXS measurements were performed (**Figure 13**). At 25 °C SAXS curves indicate the presence of nano-objects with a gyration radius of 2.2 ± 0.6 nm. As for the sample at pH 10, the scattering profile is compatible with the presence of small star-like micelles induced by the presence of the -$C_{12}H_{25}$ end group. Only small core of these highly hydrated assemblies with hydrodynamic radius about 13 nm can be detected by SAXS technique.

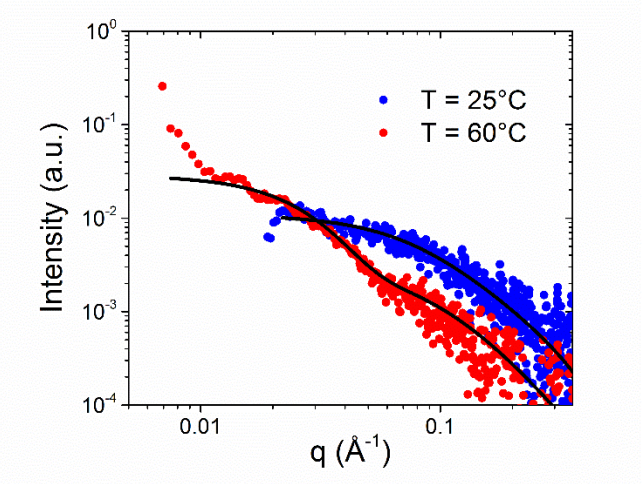

Figure 13. Small-angle X-ray scattering (SAXS) patterns recorded for 1 wt.% aqueous dispersion of PN_{5k}-*b*-PD_{5k} at 25 and 60 °C (pH = 4).

Increasing temperature to 60 °C induces an increase of overall size of the nano-objects in solution. In particular, the increase of scattering intensity at low q indicates the presence of assemblies with bigger size as compared to ones determined with our

experimental range. These big objects are in all likelihood responsible for the turbidity increase of the solution and the larger values of the hydrodynamic sizes. Possibly through SAXS results, we investigated the internal structure of these assemblies. The scattering profile could be described using a spherical form factor (**Equations** 1 to 5), which also includes an Ornstein-Zernike (OZ) type term for the scattering at high−q originating from the swollen polymer chains in good solvent (OZ exponent 1.6). These spherical aggregates at 60 °C are quite polydisperse with a radius of 5.4 ± 1.7 nm.

Turbidimetry experiments were performed using different heating rates to highlight the formation kinetics (**Figure 14A**). Decreasing heating rate causes a shift of T_c at pH 4 and a two-step process is observed whatever the heating rate (**Figure S21**). In contrast to what is observed at pH 10, the size of PN_{5k}-*b*-PD_{5k} fluctuates slightly within 2 h. Electrostatic repulsion among positive charged PD chains inhibits particle aggregation. Nevertheless, with the increase of temperature, larger aggregates are formed (**Figure 14B**).

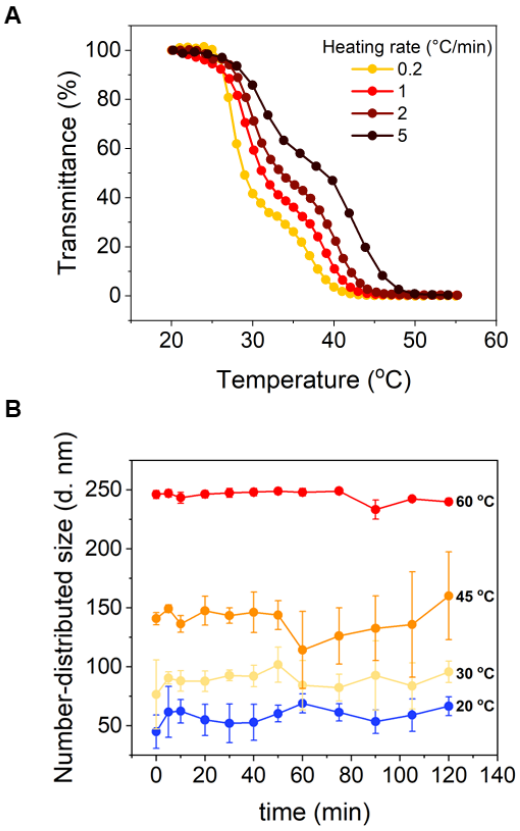

Figure 14. A. Transmittance change at different heating rates and B. Change in Number-distributed size as a function of time at 20, 30, 45 and 60 ºC of PN_{5k}-*b*-PD_{5k} at pH 4.

As above shown at pH 10, the size of obtained aggregates of PN_{5k}-*b*-PD_{5k} formed at pH 4 upon heating also depends on kinetic phenomenon due to reorganization of polymer/colloidal structure within the aggregates that occurs with characteristic timescale within minutes to hours (**Figures S22 and S23**).

c. Phase diagram of PN_{5k}-*b*-PD_{5k}.

As shown in previous sections, upon heating, a dehydration process with one single T_c is evidenced at pH 10, whereas a two-steps process seems to occur at pH 4. To gain a

further understanding, the thermoresponsive behavior of PN_{5k}-*b*-PD_{5k} at intermediate pH range were measured (**Figure 15A)**. As pH declines from 9 to 6, a single T_c decreasing from 39 to 35 °C is observed. Below pH 6, two-step transmittance change takes place in the system, which might relate to the critical role of carboxylic function: in its carboxylate form a single step process is favored, whereas the two-step process is promoted by the carboxylic form. Based on these results, a schematic phase diagram is proposed as shown in **Figure 15B**.

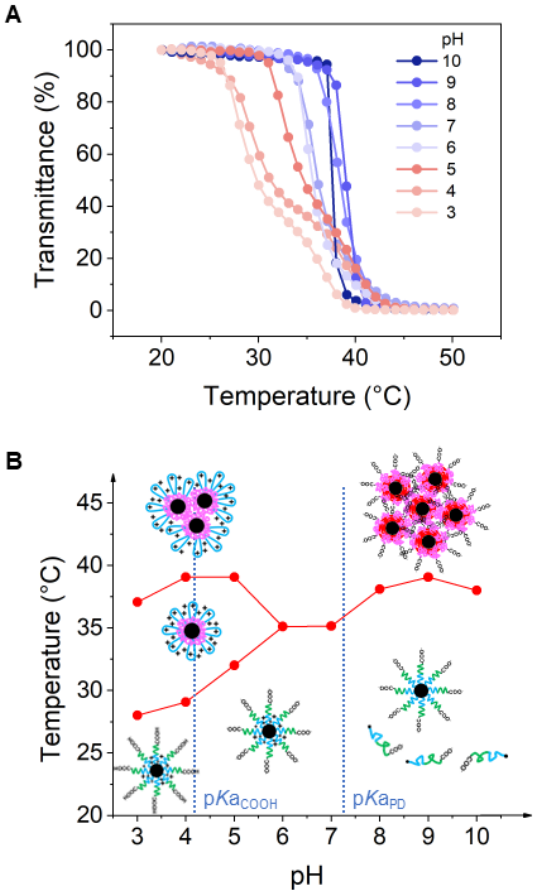

Figure 15. A. Temperature-dependent transmittance change of PN_{5k}-*b*-PD_{5k} at different pH values and B. Phase diagram of PN_{5k}-*b*-PD_{5k} solution ([PN_{5k}-*b*-PD_{5k}] = 1 wt.%, heating rate: 1 °C·min^{-1}).

d. Effect of polymer composition on thermoresponsive properties.

The effect of the copolymer composition on its behavior in solution is evaluated using the two copolymers PN_{2k}-*b*-PD_{8k} and PN_{8k}-*b*-PD_{2k}. As shown in **Figures 16** and **S24**, whatever the value of pH, PN_{8k}-*b*-PD_{2k} presents one single T_c which increases with the increase of system pH. The observed behavior seems to be mainly dictated by the majority of PNIPAM block. As previously seen for PN_{5k}-*b*-PD_{5k}, the solution behavior of PN_{2k}-*b*-PD_{8k} depends strongly on pH value. In pH range from 3 to 6, the PD block is fully protonated, while PN_{2k}-*b*-PD_{8k} solution shows two transition temperatures. As expected, the higher proportion of the PD block induced a significant increase of $T_{c,2}$ value which is measured at 49 °C at pH 4 versus 39 °C in the case of PN_{5k}-*b*-PD_{5k}. At higher pH values, only one transition is observed the value of which depends on the deprotonation level of the PD block with a significant drop since from pH 8 when the whole PD block is in its amine form.

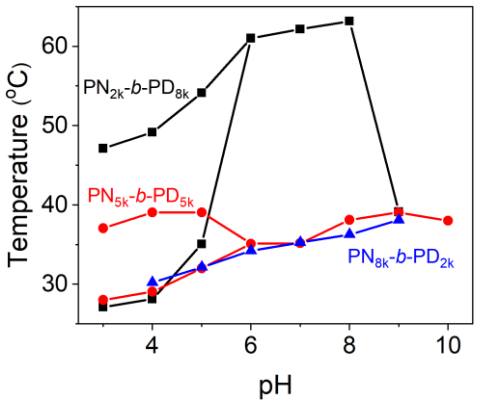

Figure 16. Cloud points of PN-*b*-PD with various compositions at different pH values (T_c determined by inflection point of transmittance curve, [PN-*b*-PD] = 1 wt.%, heating rate was 1 $^oC \cdot min^{-1}$).

TEM and DLS analyses were performed on PN_{2k}-*b*-PD_{8k} and PN_{8k}-*b*-PD_{2k} solutions and the main results are summarized in **Table S3** and **Figure 17**. As evidenced in TEM images, spherical aggregates are observed in all studied cases. Whatever the pH value, spherical aggregates are formed with larger size at temperature above T_c.

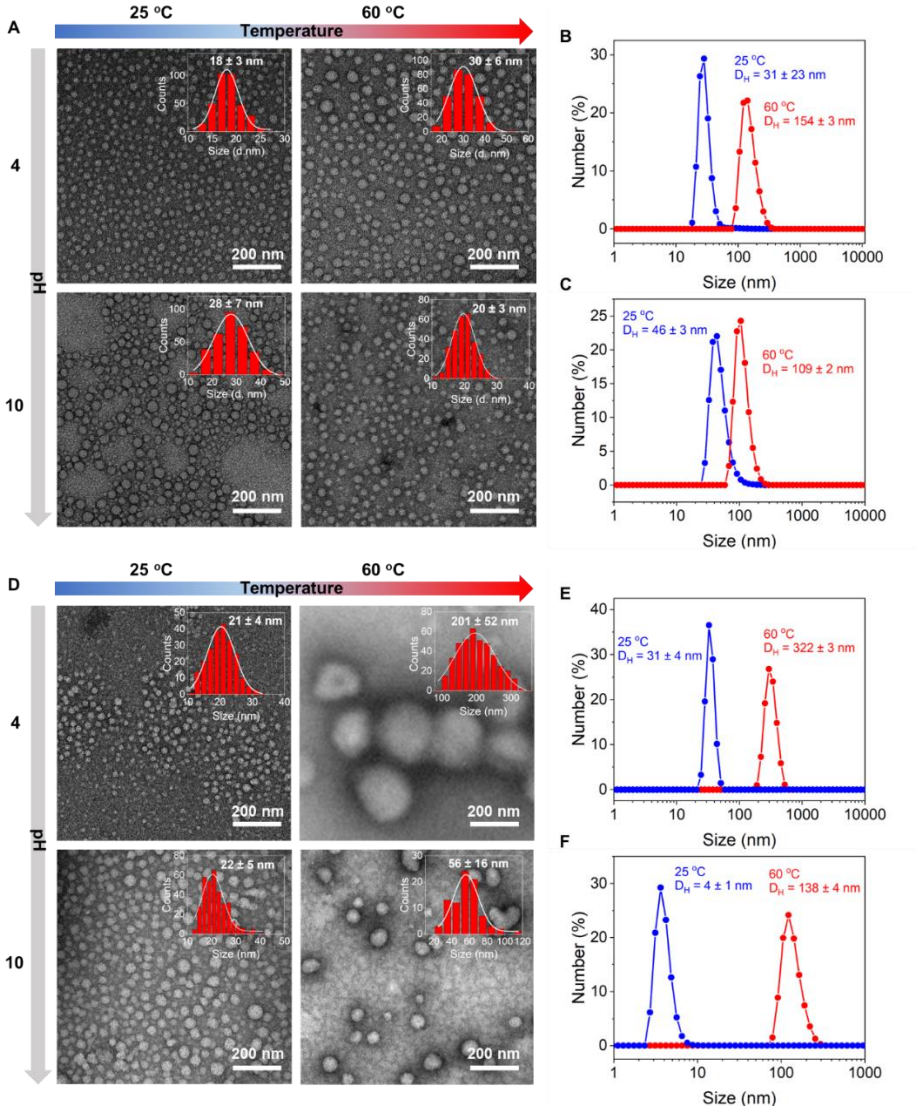

Figure 17. TEM images and Number-distributed size distribution of (A-C) PN_{2k}-*b*-PD_{8k} and (D-F) PN_{8k}-*b*-PD_{2k} at different pH values and temperatures (TEM samples were negatively stained with 2 wt.% uranyl acetate solution).

As shown in **Figure 18** (also in **Figure S25**), at 25 °C the proportion of PN has little effect on the size of the aggregates observed (around 20 nm). These aggregates result as described above from weak interactions between the PD and PN blocks in solution and are in equilibrium with free polymer chains. At 60 °C the proportion of PN has a significant effect on the size of the measured objects with a significant increase in the size of the measured objects when PN proportion increases, this increase being particularly sensitive at pH 10. At pH 4, i.e with PD in its protonated form, aggregates smaller than 110 nm are formed.

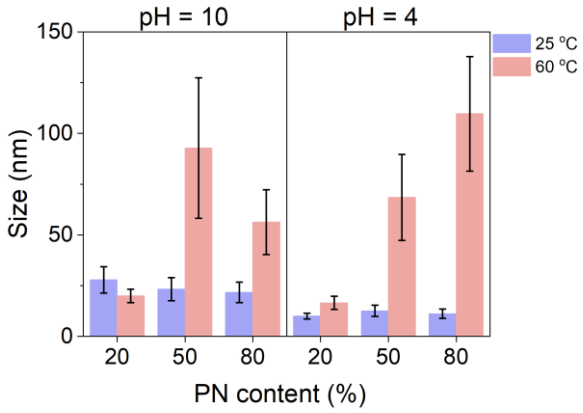

Figure 18. Evolution of particle diameter as a function of PN content at pH 4 and 10 at 25 and 60 °C (measured by TEM observation).

Conclusions

In summary, PN-*b*-PD copolymers with different compositions and corresponding homopolymers have been successfully synthesized by RAFT polymerization. The pH-switchable phase transition temperature and self-assembly behavior of these (co)polymers in aqueous solutions were studied. Functional end-groups has a key role on the aggregation properties of PN homopolymer. The properties of copolymer solutions (solubility, aggregate size) depend on both pH and copolymer composition. At pH 4, solely PN block is thermoresponsive while PD segment is hydrophilic. PN_{2k}-*b*-PD_{8k} and PN_{5k}-*b*-PD_{5k} solutions present two transition temperatures, each one inducing the formation of larger aggregates once reached with a PN positively charged outer shell. At pH 10, both PN and PD blocks are thermoresponsive. PN-*b*-PD solution has one single transition upon which larger and stable spherical nanoobjects are formed. The experiments also demonstrate the critical role of the history of the polymer in solution: the aggregation processes are particularly sensitive to kinetic considerations which explains the size variations observed at a given pH and temperature. The level of PD protonation thus allows to modulate the solution properties of PN and to obtain aggregates whose size can be limited by the presence of surface charges. Because of the possibility of modifying the level of protonation of DEAEAM monomer by acidification, but also by addition of CO_2,[27] the use of PD-based homopolymers or copolymers appears particularly interesting for many applications requiring tunable properties of these polymers at interfaces.

ASSOCIATED CONTENT

Supporting Information

The Supporting Information is available free of charge on the ACS Publications website at DOIX: XXX. Additional experimental details, materials, and methods, including NMR and FTIR spectra, DOSY measurement, SEC chromatogram, DSC thermograms of (co)polymers as well as complementary measurement on the thermoresponsive behaviour of (co)polymers.

AUTHOR INFORMATION

Corresponding Author

Jean-Daniel Marty – *Laboratoire des IMRCP, Université de Toulouse, CNRS UMR 5623, Université Toulouse III – Paul Sabatier, 118 route de Narbonne, 31062 Toulouse, France;* orcid.org/0000-0001-7631-8865; Email: Jean-daniel.marty@univ-tlse3.fr

Nancy Lauth-de Viguerie – *Laboratoire des IMRCP, Université de Toulouse, CNRS UMR 5623, Université Toulouse III – Paul Sabatier, 118 route de Narbonne, 31062 Toulouse, France;* orcid.org/0000-0002-9476-3062; Email: nancy.de-viguerie@univ-tlse3.fr

Authors

Fang Yin – *Laboratoire des IMRCP, Université de Toulouse, CNRS UMR 5623, Université Toulouse III – Paul Sabatier, 118 route de Narbonne, 31062 Toulouse, France*

Pascale Laborie – *Laboratoire des IMRCP, Université de Toulouse, CNRS UMR 5623, Université Toulouse III – Paul Sabatier, 118 route de Narbonne, 31062 Toulouse, France*

Barbara Lonetti – *Laboratoire des IMRCP, Université de Toulouse, CNRS UMR 5623, Université Toulouse III – Paul Sabatier, 118 route de Narbonne, 31062 Toulouse, France;* orcid.org/0000-0003-4291-6861

Stéphane Gineste – *Laboratoire des IMRCP, Université de Toulouse, CNRS UMR 5623, Université Toulouse III – Paul Sabatier, 118 route de Narbonne, 31062 Toulouse, France*

Yannick Coppel – *Laboratoire de Chimie de Coordination, Université de Toulouse, CNRS UPR 8241, Université Toulouse III – Paul Sabatier, 205 route de Narbonne, 31077 Toulouse, France;* orcid.org/0000-0003-0970-4082

Author Contributions

N. Lauth-de Viguerie and J.-D. Marty directed the project. F. Yin synthesized and characterized the (co)polymers, and wrote the first draft of the paper. P. Saint-Aguet contributed to the analysis of molecular weight of synthesized (co)polymers carried out on size exclusion chromatography. B. Lonetti performed SAXS measurements. S. Gineste collected the multi-angle DLS data. Y. Coppel performed NMR experiments. All authors participated in evaluating the results and gave approval to the final version of the manuscript.

Notes

The authors declare no competing financial interest.

ACKNOWLEDGMENT

The authors acknowledge financial support from the Centre national de la recherche scientifique (CNRS) and the China Scholarship Council (CSC). The authors thank S. Balor for the FF-TEM observation, B. Payré and D. Goudenèche in CMEAB center for the assistance with TEM experiments and P. Roblin for the access to SAXS facilities.

ABBREVIATIONS

PN-*b*-PD: poly(*N*-isopropylacrylamide)-block-poly(*N*,*N*-diethylamino ethyl acrylamide) (PNIPAM-*b*-PDEAEAM)

REFERENCES

(1) Xiao, Z.-P.; Yang, K.-M.; Liang, H.; Lu, J. Synthesis of Magnetic, Reactive, and Thermoresponsive Fe_3O_4 Nanoparticles via Surface-Initiated RAFT Copolymerization of *N*-Isopropylacrylamide and Acrolein. *J. Polym. Sci. A Polym. Chem.* **2010**, *48*, 542–550.

(2) Schattling, P.; Jochum, F. D.; Theato, P. Multi-stimuli responsive polymers – the all-in-one talents. *Polym. Chem.* **2014**, *5*, 25–36.

(3) Gil, E. S.; Hudson, S. M. Stimuli-reponsive polymers and their bioconjugates. *Prog. Polym. Sci.* **2004**, *29*, 1173–1222.

(4) Kocak, G.; Tuncer, C.; Bütün, V. pH-Responsive polymers. *Polym. Chem.* **2017**, *8*, 144–176.

(5) Ulijn, R. V. Enzyme-responsive materials: a new class of smart biomaterials. *J. Mater. Chem.* **2006**, *16*, 2217–2225.

(6) Hu, J.; Zhang, G.; Liu, S. Enzyme-responsive polymeric assemblies, nanoparticles and hydrogels. *Chem. Soc. Rev.* **2012**, *41*, 5933–5949.

(7) Roy, D.; Brooks, W. L. A.; Sumerlin, B. S. New directions in thermoresponsive polymers. *Chem. Soc. Rev.* **2013**, *42*, 7214–7243.

(8) Liu, R.; Fraylich, M.; Saunders, B. R. Thermoresponsive copolymers: from fundamental studies to applications. *Colloid Polym. Sci.* **2009**, *287*, 627–643.

(9) Dimitrov, I.; Trzebicka, B.; Müller, A. H. E.; Dworak, A.; Tsvetanov, C. B. Thermosensitive water-soluble copolymers with doubly responsive reversibly interacting entities. *Prog. Polym. Sci.* **2007**, *32*, 1275–1343.

(10) Schild, H. G. Poly(*N*-isopropylacrylamide): experiment, theory and application. *Prog. Polym. Sci.* **1992**, *17*, 163–249.

(11) Scarpa, J. S.; Mueller, D. D.; Klotz, I. M. Slow Hydrogen-Deuterium Exchange in a Non-*α*-helical Polyamide. *J. Am. Chem. Soc.* **1967**, *89*, 6024–6030.

(12) Laukkanen, A.; Valtola. L.; Winnik, F. M.; Tenhu, H. Formation of Colloidally Stable Phase Separated Poly(*N*-vinylcaprolactam) in Water: A Study by Dynamic Light

Scattering, Microcalorimetry, and Pressure Perturbation Calorimetry. *Macromolecules* **2004**, *37*, 2268–2274.

(13) Beija, M.; Marty, J.-D.; Destarac, M. Thermoresponsive poly(*N*-vinyl caprolactam)-coated gold nanoparticles: sharp reversible response and easy tunability. *Chem. Commun.* **2011**, *47*, 2826–2828.

(14) Zhao, X.; Coutelier, O.; Nguyen, H. H.; Delmas, C.; Destarac, M.; Marty, J.-D. Effect of copolymer composition of RAFT/MADIX-derived *N*-vinylcaprolactam/*N*-vinylpyrrolidone statistical copolymers on their thermoresponsive behavior and hydrogel properties. *Polym. Chem.* **2015**, *6*, 5233–5243.

(15) Yin, F.; Nguyen, H. H.; Coutelier, O.; Destarac, M.; Lauth-de Viguerie, N.; Marty, J.-D. Effect of copolymer composition of controlled (*N*-vinylcaprolactam/*N*-vinylpyrrolidone) statistical copolymers on formation, stabilization, thermoresponsiveness and catalytic properties of gold nanoparticles. *Colloids Surf. A Physicochem. Eng. Asp.* **2021**, *630*, 127611.

(16) Persson, J.; Johansson, H.-O.; Galaev, I.; Mattiasson, B.; Tjerneld, F. Aqueous polymer two-phase systems formed by new thermoseparating polymers. *Bioseparation* **2000**, *9*, 105–116.

(17) Pang, B.; Yu, Y.; Zhang, W. Thermoresponsive Polymers Based on Tertiary Amine Moieties. *Macromol. Rapid Commun.* **2021**, *42*, 2100504.

(18) Hils, C.; Fuchs, E.; Eger, F.; Schöbel, J.; Schmalz, H. Converting Poly(Methyl Methacrylate) into a Triple-Responsive Polymer. *Chem. Eur. J.* **2020**, *26*, 5611–5614.

(19) Wang, K.; Song, Z.; Liu, C.; Zhang, W. RAFT synthesis of triply responsive poly[*N*-[2-(dialkylamino)ethyl]acrylamide]s and their *N*-substitute determined response. *Polym. Chem.* **2016**, *7*, 3423–3433.

(20) Thavanesan, T.; Herbert, C.; Plamper, F. A. Insight in the Phase Separation Peculiarities of Poly(dialkylaminoethyl methacrylate)s. *Langmuir* **2014**, *30*, 5609–5619.

(21) Dubruel, P.; Schacht, E. Vinyl Polymers as Non-Viral Gene Delivery Carriers: Current Status and Prospects. *Macromol. Biosci.* **2006**, *6*, 789–810.

(22) Li, L.; Wei, Y.; Gong, C. Polymeric Nanocarriers for Non-Viral Gene Delivery. *J. Biomed. Nanotechnol.* **2015**, *11*, 739–770.

(23) Kim, K.; Chen, W. C. W.; Heo, Y.; Wang, Y. Polycations and their biomedical applications. *Prog. Polym. Sci.* **2016**, *60*, 18–50.

(24) Giaouzi, D.; Pispas, S. PNIPAM-b-PDMAEA double stimuli responsive copolymers: Effects of composition, end groups and chemical modification on solution self-assembly. *Eur. Polym. J.* **2020**, *135*, 109867.

(25) Zhang, Y.; Wu, T.; Liu, S. Micellization Kinetics of a Novel Multi-Responsive Double Hydrophilic Diblock Copolymer Studied by Stopped-Flow pH and Temperature Jump. *Macromol. Chem. Phys.* **2007**, *208*, 2492–2501.

(26) Smith, A. E.; Xu, X.; Kirkland-York, S. E.; Savin, D. A.; McCormick, C. L. "Schizophrenic" Self-Assembly of Block Copolymers Synthesized via Aqueous RAFT Polymerization: From Micelles to Vesicles. *Macromolecules* **2010**, *43*, 1210–1217.

(27) Song, Z.; Wang, K.; Gao, C.; Wang, S.; Zhang, W. A New Thermo-, pH-, and CO2-Responsive Homopolymer of Poly[N-[2-(diethylamino)ethyl]acrylamide]: Is the Diethylamino Group Underestimated? *Macromolecules* **2016**, *49*, 162–171.

(28) Simonova, M. A.; Khairullin, A. R.; Tyurina, V. O.; Filippov, A. P.; Sadikov, A. Y.; Kamorin, D. M.; Kamorina, S. I. Self-Organization Processes in Poly(*N*-[2-(diethylamino)ethyl]acrylamide) Buffer Solutions with Change in Concentration and pH of a Medium. *Polym. Sci. Ser. A*+ **2020**, *62*, 24–31.

(29) Guan, X.; Meng, L.; Jin, Q.; Lu, B.; Chen, Y.; Li, Z.; Wang, L.; Lai, S.; Lei, Z. A New Thermo-, pH- and CO_2-Responsive Fluorescent Four-Arm Star Polymer with Aggregation-Induced Emission for Long-Term Cellular Tracing. *Macromol. Mater. Eng.* **2018**, *303*, 1700553.

(30) Lee, J.; Ku, K. H.; Park, C. H.; Lee, Y. J.; Yun, H.; Kim, B. J. Shape and Color Switchable Block Copolymer Particles by Temperature and pH Dual Responses. *ACS Nano* **2019**, *13*, 4230–4237.

(31) Till, U.; Gaucher, M.; Amouroux, B.; Gineste, S.; Lonetti, B.; Marty, J.-D.; Mingotaud, C.; Bria, C. R. M.; Williams, S. K. R.; Violleau, F.; Mingotaud, A. F. Frit inlet field-flow fractionation techniques for the characterization of polyion complex self-assemblies. *J. Chromatogr. A* **2017**, *1481*, 101–110.

(32) Richter, D.; Farago, B.; Huang, J. S.; Fetters, L. J.; Ewen, B. A Study of Single-Arm Relaxation in a Polystyrene Star Polymer by Neutron Spin Echo Spectroscopy. *Macromolecules* **1989**, *22*, 468–472.

(33) RAFT Polymerization: Methods, Synthesis, Applications; Moad, G.; Rizzardo, E. (Eds.) Wiley: Weinheim, Germany, 2022.

(34) Wang, M.; Marty, J.-D.; Destarac, M. Xanthates in RAFT polymerization. In *RAFT Polymerization. Methods, Synthesis, Applications*; Moad, G., Rizzardo, E., Eds.; Wiley-VCH: Weinheim, Germany, **2022**; Volume 2, pp. 493–548.

(35) Moad, G. Trithiocarbonates in RAFT polymerization. In *RAFT polymerization. Methods, Synthesis, Applications*; Moad, G., Rizzardo, E., Eds.; Wiley-VCH: Weinheim, Germany, 2022; Volume 2, pp. 359–492

(36) Sharker, K. K.; Takeshima, S.; Toyama, Y.; Ida, S.; Kanaoka, S.; Yusa, S.-i. pH- and thermo-responsive behavior of PNIPAM star containing terminal carboxy groups in aqueous solutions. *Polymer* **2020**, *203*, 122735.

(37) Narrainen, A. P.; Pascual, S.; Haddleton, D. M. Amphiphilic Diblock, Triblock, and Star Block Copolymers by Living Radical Polymerization: Synthesis and Aggregation Behavior. *J. Polym. Sci. A Polym. Chem.* **2002**, *40*, 439–450.

(38) Sistach, S.; Beija, M.; Rahal, V.; Brûlet, A.; Marty, J.-D.; Destarac, M.; Mingotaud, C. Thermoresponsive Amphiphilic Diblock Copolymers Synthesized by MADIX/RAFT: Properties in Aqueous Solutions and Use for the Preparation and Stabilization of Gold Nanoparticles. *Chem. Mater.* **2010**, *22*, 3712–3724.

(39) Nguyen, H. H.; Brûlet, A.; Goudounèche, D.; Saint-Aguet, P.; Lauth-de Viguerie, N.; Marty, J.-D. The effect of polymer branching and average molar mass on the formation, stabilization and thermoresponsive properties of gold nanohybrids stabilized by poly(*N*-isopropylacrylamides). *Polym. Chem.* **2015**, *6*, 5838–5850.

(40) Plummer, R.; Hill, D. J. T.; Whittaker, A. K. Solution Properties of Star and Linear Poly(*N*-isopropylacrylamide). *Macromolecules* **2006**, *39*, 8379–8388.

(41) Nadal, C.; Gineste, S.; Coutelier, O.; Tourrette, A.; Marty, J.-D.; Destarac, M. A deeper insight into the dual temperature- and pH-responsiveness of poly(vinylamine)-b-poly(*N*-isopropylacrylamide) double hydrophilic block copolymers. *Colloids Surf. A Physicochem. Eng. Asp.* **2022**, *641*, 128502.

(42) Read, E.; Lonetti, B.; Gineste, S.; Sutton, A. T.; Di Cola, E.; Castignolles, P.; Gaborieau, M.; Mingotaud, A. F.; Destarac, M.; Marty, J.-D. Mechanistic insights into the formation of polyion complex aggregates from cationic thermoresponsive diblock copolymers. *J. Colloid Interf. Sci.* **2021**, *590*, 268–276.

(43) Yin, F.; Behra, J. S.; Beija, M.; Brûlet, A.; Fitremann, J.; Payré, B.; Gineste, S.; Destarac, M.; Lauth-de Viguerie, N.; Marty, J.-D. Effect of the microstructure of *n*-butyl acrylate/*N*-isopropylacrylamide copolymers on their thermo-responsiveness, self-organization and gel properties in water. *J. Colloid Interf. Sci.* **2020**, *578*, 685–697.

(44) FitzGerald, P. A.; Gupta, S.; Wood, K.; Perrier, S.; Warr, G. G. Temperature- and pH-Responsive Micelles with Collapsible Poly(*N*-isopropylacrylamide) Headgroups. *Langmuir* **2014**, *30*, 7986–7992.

(45) Xia, Y.; Burke, N. A. D.; Stöver, H. D. H. End Group Effect on the Thermal Response of Narrow-Disperse Poly(*N*-isopropylacrylamide) Prepared by Atom Transfer Radical Polymerization. *Macromolecules* **2006**, *39*, 2275–2283.

(46) Škvarla, J.; Raya, R. K.; Uchman, M.; Zedník, J.; Procházka, K.; Garamus, V. M.; Meristoudi, A.; Pispas, S.; Štěpánek, M. Thermoresponsive behavior of poly(*N*-

isopropylacrylamide)s with dodecyl and carboxyl terminal groups in aqueous solution: pH-dependent cloud point temperature. *Colloid Polym. Sci.* **2017**, *295*, 1343–1349.

(47) Van de Wetering, P.; Moret, E. E.; Schuurmans-Nieuwenbroek, N. M. E.; Van Steenbergen, M. J.; Hennink, W. E. Structure-Activity Relationships of Water-Soluble Cationic Methacrylate/Methacrylamide Polymers for Nonviral Gene Delivery. *Bioconjugate Chem.* **1999**, *10*, 589−597.

(48) Patterson, J. P.; Kelley, E. G.; Murphy, R. P.; Moughton, A. O.; Robin, M. P.; Lu, A.; Colombani, O.; Chassenieux, C.; Cheung, D.; Sullivan, M. O.; Epps, T. H.; O'Reilly, R. K. Structural Characterization of Amphiphilic Homopolymer Micelles Using Light Scattering, SANS, and Cryo-TEM. *Macromolecules* **2013**, *46*, 6319–6325.

(49) Ohnsorg, M. L.; Ting, J. M.; Jones, S. D.; Jung, S.; Bates, F. S.; Reineke, T. M.; Tuning PNIPAm self-assembly and thermoresponse: roles of hydrophobic end-groups and hydrophilic comonomer. *Polym. Chem.* **2019**, *10*, 3469–3479.